# G Protein-Coupled Receptor Kinase-2 (GRK-2) controls exploration through neuropeptide signaling in *Caenorhabditis elegans*

Kristen Davis[1,2,3], Christo Mitchell[4,+], Olivia Weissenfels[4,+], Jihong Bai[5], David M. Raizen[1,6], Michael Ailion[4,*], and Irini Topalidou[4,5,*]

[1]Department of Neurology, Perelman School of Medicine, University of Pennsylvania, Philadelphia, PA, USA

[2]Center for Excellence in Environmental Toxicology (CEET), Perelman School of Medicine, University of Pennsylvania, Philadelphia, PA, USA

[3]Department of Neuroscience, Vickie and Jack Farber Institute of Neuroscience, Thomas Jefferson University, Philadelphia, PA, USA

[4]Department of Biochemistry, University of Washington, Seattle, WA, USA

[5]Fred Hutchinson Cancer Center, Seattle, WA, USA

[6]Chronobiology and Sleep Institute, Perelman School of Medicine, University of Pennsylvania, Philadelphia, PA, USA.

[+]These authors contributed equally to this work

[*]Corresponding authors

Email: etopalid@fredhutch.org

Email: mailion@uw.edu

Short title: GRK-2 controls exploration and movement quiescence

## Abstract

Animals alter their behavior in manners that depend on environmental conditions as well as their developmental and metabolic states. For example, *C. elegans* is quiescent during larval molts or during conditions of satiety. By contrast, worms enter an exploration state when removed from food. Sensory perception influences movement quiescence (defined as a lack of body movement), as well as the expression of additional locomotor states in *C. elegans* that are associated with increased or reduced locomotion activity, such as roaming (exploration behavior) and dwelling (local search). Here we find that movement quiescence is enhanced, and exploration behavior is reduced in G protein-coupled receptor kinase *grk-2* mutant animals. *grk-2* was previously shown to act in chemosensation, locomotion, and egg-laying behaviors. Using neuron-specific rescuing experiments, we show that GRK-2 acts in multiple ciliated chemosensory neurons to control exploration behavior. *grk-2* acts in opposite ways from the cGMP-dependent protein kinase gene *egl-4* to control movement quiescence and exploration behavior. Analysis of mutants with defects in ciliated sensory neurons indicates that *grk-2* and the cilium-structure mutants act in the same pathway to control exploration behavior. We find that GRK-2 controls exploration behavior in an opposite manner from the neuropeptide receptor NPR-1 and the neuropeptides FLP-1 and FLP-18. Finally, we show that secretion of the FLP-1 neuropeptide is negatively regulated by GRK-2 and that overexpression of FLP-1 reduces exploration behavior. These results define neurons and molecular pathways that modulate movement quiescence and exploration behavior.

## Author summary

Many modulatory neurotransmitters affect behavior by binding to G protein-coupled receptors (GPCRs) and initiating signals that modify neuronal activity. GPCRs are regulated by G protein-coupled receptor kinases (GRKs). GRKs phosphorylate and promote the inactivation of GPCRs. Here we identify GRK-2 as a regulator of distinct locomotor states in *C. elegans*. We find that GRK-2 acts in olfactory sensory neurons to promote exploration and suppress movement quiescence. Additionally, we show that GRK-2 acts in opposition to a neuropeptide signaling pathway that acts in interneurons. Thus, this study demonstrates critical roles for GRK-2 in regulating neuromodulatory signaling and locomotor behavior.

## Introduction

Animals modify their behaviors in response to changes in their environment or metabolic state. Sensory and neuromodulatory signals play a major role in adapting behavior to environmental or metabolic changes [1-6]. For example, animals experience periods of quiescence and arousal that depend on sensory and neuromodulatory cues [3,5,7-9]. Arousal is a state of increased responsiveness that can be associated with fear or starvation, whereas quiescence is characterized by decreased responsiveness and is associated with sleep and satiety. Even though sensory and neuromodulatory signals are recognized as major modulators of behavior, the precise mechanisms that mediate behavioral strategies under different inputs remain largely unknown. Here we describe how a locomotor behavior in the nematode *Caenorhabditis elegans* is altered through the action of the G protein-coupled receptor kinase-2 (GRK-2) in sensory neurons and neuromodulator signaling in interneurons.

Several examples of movement quiescence in response to changes in the external environment or the internal metabolic state of the animal have been reported in *C. elegans. C. elegans* enters an exploration state when it is removed from food [10,11] and becomes quiescent during molting or under conditions of prolonged starvation, satiety, or cellular stress [3,12-17]. Sensory perception affects quiescence, as well as additional locomotor states in *C. elegans* that are characterized by increased or reduced locomotion activity, such as roaming/exploration and dwelling [2]. The animal covers a large area during roaming (exploring), while it restricts its activity to a small region during the dwelling state. The mechanism by which sensory perception modulates this locomotor strategy is unknown.

Quiescence, roaming, and dwelling are controlled by the function of the cGMP-dependent protein kinase (PKG) gene *egl-4* in sensory neurons. *egl-4* loss-of-function mutant animals have chemosensory defects [18] and attenuated sensory adaptation [19]. EGL-4 is a regulator of lethargus quiescence, a sleep-like behavior that takes place during molts [3], and of a satiety-induced sleep-like behavior [12]. EGL-4 also defines the time the animals spend

85 roaming and dwelling since *egl-4* loss of function mutant animals show increased exploration
86 [2,20]. Here, we describe a role for GRK-2 in the sensory neurons of *C. elegans* to regulate
87 movement quiescence and exploration in an opposite manner to EGL-4.

88 GRKs play key roles in attenuating the strength of neuromodulatory pathways by
89 phosphorylating G protein-coupled receptors (GPCRs) and promoting the inactivation of GPCR
90 signaling [21]. Vertebrates have seven GRKs that are classified into three subfamilies: the visual
91 GRKs (GRK1/7), the GRK2/3 subfamily, and the GRK4/5/6 subfamily [22]. *C. elegans,* which
92 lacks a visual system, has GRK-1 and GRK-2, which are orthologs of the mammalian GRK4/5/6
93 and GRK2/3 families, respectively [23,24]. *grk-2* is expressed broadly in the nervous system
94 and has a broad impact on animal physiology including chemosensation [23], gustatory
95 plasticity [25], egg-laying [26], crawling [27], swimming [27,28], and oxidative and heat stress
96 responses [29,30]. Elimination of *grk-2* function renders animals unable to respond to a wide
97 range of chemical stimuli, suggesting that GRK-2 plays a positive role in chemosensation [23].
98 Similarly, *grk-2* mutant animals show reduced crawling rates and are unable to swim, again
99 suggesting that GRK-2 plays a positive role in regulating crawling and swimming [27,28]. GRK-2
100 was proposed to promote crawling and swimming by negatively regulating the D2-like dopamine
101 receptor DOP-3 [27,28]. GRK-2 regulates chemosensation by acting in sensory neurons [23],
102 but it controls crawling and swimming by acting in premotor interneurons [27,28], suggesting
103 that GRK-2 acts in different neurons to modulate distinct behavioral outcomes.

104 Besides sensory perception, neuromodulation has also been shown to play a critical role
105 in defining arousal and quiescence as well as roaming and dwelling in *C. elegans*. For example,
106 mutants lacking the neuropeptide receptor NPR-1 have been used as a model for studying
107 arousal since both lethargus and movement quiescence are reduced in *npr-1* mutants [8,31-33].
108 Specifically, increased RMG interneuron activity in *npr-1* mutant animals during lethargus
109 induces secretion of the neuropeptide pigment dispersing factor PDF-1, resulting in increased
110 animal motility and reduced quiescence [31]. PDF-1 also positively regulates roaming, whereas

111 serotonin plays an opposite role by increasing dwelling [4]. Here we find that GRK-2 controls
112 exploration in an opposite manner to NPR-1 and the neuropeptides FLP-1 and FLP-18. We also
113 show that GRK-2 acts in different pathways than PDF and serotonergic signaling. Finally, we
114 demonstrate that secretion of FLP-1, a neuropeptide that regulates locomotion [34-37], depends
115 on GRK-2 and that overexpression of *flp-1* inhibits exploration behavior.
116

## Results

### *grk-2* mutants have exploration and dispersal defects

Our previous work suggested that GRK-2 positively regulates crawling and swimming by negatively regulating the D2-like dopamine receptor DOP-3 [27,28]. *grk-2(gk268)* null mutant animals exhibit slow crawling and impaired swimming, and mutations in *dop-3* suppress both these phenotypes. *grk-2* mutant animals also have a decreased exploration behavior: they restrict their movements to a limited region of the bacterial lawn, whereas wild-type animals explore the entire lawn [27]. This exploration behavior defect could be due to decreased roaming, increased dwelling, or increased quiescence. We used simple radial locomotion and exploration assays ([4,38]; see also Methods) to quantify this phenotype by observing the radial distance that individual animals traveled over 1 h (Fig 1A) or the tracks that individual animals left on a lawn of *E. coli* over an 18-20 hr period (Fig 1D). We found that *grk-2(gk268)* mutant animals disperse and explore less compared to wild-type (Fig 1B and 1E). This phenotype is independent of sex since *grk-2* males also explore less than wild type males (Fig 1F). To examine whether the *grk-2* dispersal defect depends on the presence of food we performed the dispersal assay on plates without *E. coli.* We found that *grk-2(gk268)* mutant animals disperse less compared to wild type even in the absence of the bacteria lawn (Fig 1C), suggesting that the dispersal defect of *grk-2* mutant is independent of the presence or absence of food.

Although the *dop-3(vs106)* mutation suppresses the slow locomotion and swimming defects of *grk-2(gk268)* mutant animals [27,28], it did not significantly alter the dispersal or exploration behavior of *grk-2(gk268)* (Fig 1B,C and E), suggesting that GRK-2 affects the exploration behavior independently of DOP-3, and that the mechanism by which GRK-2 influences exploration behavior is different than its role in regulating crawling and swimming.

### GRK-2 acts in a different pathway than serotonergic or PDF signaling to affect exploration

143 Worm exploration behavior is regulated by serotonergic and PDF signaling: serotonin
144 inhibits exploration through the MOD-1 serotonin-gated chloride channel, while PDF-1 promotes
145 exploration through the Gαs-coupled PDF receptor PDFR-1 [4]. To examine whether GRK-2
146 acts in the PDF-1 pathway to affect the exploration behavior we compared animals that were
147 mutant for both *grk-2* and *pdfr-1* to single mutants. We found that *pdfr-1(ok3425)* mutant
148 animals display decreased exploration, as previously reported [4] and that the phenotype of the
149 double mutant *grk-2(gk268); pdfr-1(ok3425)* is stronger than the phenotype of the single
150 mutants (Fig S1A), suggesting that GRK-2 and PDFR-1 act in different pathways to control
151 exploration. Similarly, to examine whether GRK-2 acts in the serotonin pathway to control
152 exploration, we built double mutants between *grk-2* and *tph-1* mutants (*tph-1* encodes the rate-
153 limiting enzyme for serotonin synthesis). We verified that *tph-1(mg280)* mutant animals display
154 increased exploration [4] and further showed that *grk-2(gk268); tph-1(mg280)* double mutant
155 animals have an intermediate phenotype between that of either *grk-2* or *tph-1* single mutants
156 (Fig S1B), suggesting that *grk-2* and *tph-1* act in separate pathways to control exploration. Our
157 results imply that GRK-2 acts in a different pathway than serotonergic or PDF signaling to affect
158 the exploration behavior.
159
160 **GRK-2 functions in the ciliated neurons to affect the exploration behavior**
161 GRK-2 is expressed broadly in the nervous system [23] and acts in premotor
162 interneurons to control crawling and swimming [27,28]. To determine where GRK-2 acts to
163 affect the exploration behavior, we expressed the *grk-2* cDNA under the control of neuron-
164 specific promoters. Expression of *grk-2* cDNA under the pan-neuronal promoter (*rab-3p*) fully
165 rescued the *grk-2(gk268)* mutant exploration defect but expression in ventral cord acetylcholine
166 motor neurons alone (using the *acr-2* promoter) or in command interneurons alone (using the
167 *nmr-1* promoter) did not rescue this defect (Fig 2A). Expression of *grk-2* cDNA in the same set
168 of command interneurons rescued the crawling defects of *grk-2* mutant animals (Fig S2),

169 supporting the notion that the role that GRK-2 plays to affect the exploration behavior is different
170 from its role in crawling.

171 *grk-2* mutants fail to respond to a wide range of chemical stimuli, suggesting that GRK-2
172 is a positive regulator of chemosensation [23]. To test the hypothesis that the exploration defect
173 in *grk-2(gk268)* mutant animals is explained by its role in chemosensation, we expressed the
174 *grk-2* cDNA under the ciliated sensory neuron promoters *xbx-1p* and *osm-6p*. Expression of *grk-*
175 *2* cDNA in ciliated sensory neurons fully rescued the exploration defect of *grk-2* mutant animals
176 both in the presence and absence of food (Fig 2B,C). Our result that transgenic expression of
177 *grk-2* under *rab-3, xbx-1*, or *osm-6* heterologous promoters fully rescued the *grk-2* exploration
178 defect (Fig 2A-C) suggests that the precise level of GRK-2 is not critical to its function.

179 To further narrow down the site of action of GRK-2 in exploration behavior we expressed
180 the *grk-2* cDNA under the control of the *odr-3* promoter (*odr-3p*), which promotes expression in
181 olfactory and nociceptive neurons: AWA, AWB, AWC, ASH, and ADF [39]. Expression of *grk-2*
182 under the *odr-3* promoter partially rescued the exploration defect of *grk-2* mutant animals,
183 suggesting that *grk-2* acts in multiple ciliated neurons to affect exploration behavior (Fig 2D). An
184 operon GFP was included in the expression construct downstream of the 3'UTR allowing
185 confirmation of expression (see Methods). To confirm that *grk-2* is expressed in *odr-3-*
186 expressing neurons, we expressed the cDNA encoding GRK-2 protein fused to tagRFP (*grk-*
187 *2*::tagRFP) under the *grk-2* promoter as well as mNeon::NLS driven by the *odr-3* promoter (*odr-*
188 *3p*::mNeon::NLS). We confirmed that *grk-2* is indeed expressed in *odr-3*-expressing neurons
189 (shown with arrows in Fig 2G).

190 To dissect further the subset of chemosensory neurons where GRK-2 acts to control
191 exploration behavior we expressed the *grk-2* cDNA under the control of the *sra-6* promoter,
192 which is primarily expressed in the ASH and ASI chemosensory neurons (*sra-6p*; [40]).
193 Expression of *grk-2* under the *sra-6* promoter partially rescued the *grk*-2 exploration defect,
194 suggesting that a part of GRK-2's role in exploration behavior is due to its action in the ASH or

195 ASI neurons (Fig 2E). Similarly, *grk-2* expression in the AWA, AWB, or AWC neurons (*odr-10p*:
196 expression in AWA [41]; *str-1p*: expression in AWB [42]; *str-2p*: expression in AWC-ON [43])
197 only slightly rescued the *grk-2* exploration defect (Fig 2F). Even *grk-2* expression under the
198 combined control of the *odr-1, str-1,* and *str-2* promoters only partially rescued the *grk-2*
199 exploration defect (Fig 2E), again suggesting that *grk-2* acts in more than a single type of
200 ciliated neuron to control exploration behavior. To address the possibility that expression of *grk-*
201 *2* in any ciliated sensory neuron might rescue the exploration defect of *grk-2* mutant animals, we
202 expressed *grk-2* under the *gcy-8* promoter, which is solely expressed in the AFD thermosensory
203 neurons (*gcy-8p;* [44]). Expression of *grk-2* under the *gcy-8* promoter failed to rescue the *grk-2*
204 exploration defect (Fig 2H). Similarly, expression of *grk-2* under the dopaminergic neuron
205 promoter *dat-1* [45] failed to rescue the *grk-2* exploration defect (*dat-1p*; Fig 2I).
206 To examine whether GRK-2 plays a developmental role to affect exploration we placed
207 *grk-2* cDNA under the control of a heat shock-inducible promoter and introduced it in *grk-2*
208 mutant animals. Heat shock in adult animals partially but significantly restored the exploration
209 behavior of *grk-2* (Fig 2J). These results together suggest that GRK-2 has a functional role in
210 mature ciliated sensory neurons that affect the exploration behavior.
211
212 **Mutants in cilia-related genes have exploration defects similar to *grk-2***
213 Mutants with defects in sensory perception exhibit exploration defects on food like the
214 ones described here for *grk-2* [2]. Specifically, mutants with cilium-structure defects (such as
215 *che-2*) restrict their movements to a limited region of the bacterial lawn, while sensory signal
216 transduction mutants like *tax-2* and *tax-4* have a weaker defect than cilium-structure mutants
217 [2]. *grk-2* mutant animals are not defective in their ability to take up a fluorescent dye like the
218 cilium-structure mutants (Dye-filling assay; [23]), an assay indicative of the structural integrity of
219 the sensory cilia. To confirm that cilium structure mutants have exploration defects similar to
220 *grk-2*, we performed the exploration assay on *che-2(e1033)* and *daf-10(e1387)* mutant animals

221 in the presence or absence of food. We found that *che-2(e1033)* and *daf-10(e1387)* mutant
222 animals are exploration defective identical to *grk-2(gk268*) (Fig 3A-C). Additionally, the *che-*
223 *2(e1033)* and *daf-10(e1387)* mutations do not enhance the phenotype of *grk-2* mutant (Fig 3A-
224 C). The lack of an obvious enhancement is not due to a floor effect since *grk-2; pdfr-1* double
225 mutant animals have stronger exploration phenotype than the single mutants (Fig S1A). These
226 findings suggest that *che-2, daf-10*, and *grk-2* act in the same pathway to control exploration
227 (Fig 3A-C).

228 To further investigate which kinds of sensory perception affect exploration, we used the
229 exploration assay to test mutants with different sensory defects. Most chemosensory and
230 osmosensory- defective mutants that possess defective cilia based on their Dye filling
231 phenotype [46] had defects in exploration (Fig 3D). Specifically, mutants with strong cilium-
232 structure defects (shown in blue in Fig 3D) had strong exploration defects and most mutants
233 with weak cilium defects (shown in green in Fig 3D) had weaker exploration defects. Other
234 chemosensory, osmosensory, and thermosensory defective mutants (*odr-1, odr-3, odr-8, odr-*
235 *10, osm-7, osm-10, tax-2, tax-4, ttx-1(p767*), also had exploration defects but not as severe as
236 *grk-2*. Interestingly, chemosensory and osmosensory mutants *che-1, che-6, che-7, odr-2, odr-4,*
237 *odr-5, odr-7, osm-9,* and *osm-11*, as well as thermosensory *ttx-1(oy26* and *oy29)* mutants were
238 not significantly defective. Surprisingly, the *ocr-2* canonical null mutant *ak47* (VM396 strain)
239 showed an exploration defect that was not observed with the *ocr-2(ok1711)* allele (VC1233
240 strain). Given that *ok1711* contains a deletion of at least three exons it is presumably a null
241 allele, suggesting that either the VC1233 *ocr-2*(*ok1711)* strain has a suppressor mutation that
242 rescues the exploration defect or that the VM396 *ocr-2(ak47)* strain has an exploration defect
243 due to a background mutation and not because of the *ocr-2(ak47)* deletion. To distinguish
244 between these possibilities, we outcrossed strains VC1233 and VM396 and tested the
245 exploration behavior of outcrossed strains BJH2762 *ocr-2(ok1711)* and BJH2763 *ocr-2(ak47)*.
246 We found that strain BJH2763 *ocr-2(ak47)* did not have an exploration defect, suggesting that

247 the *ocr-2(ak47)* mutation does not cause exploration defects and that strain VM396 has a
248 background mutation that makes the animals exploration defective (Fig S3A). Notably, oxygen-
249 sensing mutant *gcy-35* and mechanosensory-defective mutants *mec-3, mec-4,* and *glr-1* did not
250 show exploration defects. We conclude that ciliated neurons that are involved in
251 chemosensation and osmosensation play a significant role in the exploration behavior.
252

253 **GRK-2 controls movement quiescence in an opposite way to EGL-4**

254 *C. elegans* locomotory behavior in the presence of food alternates between two discrete
255 states called roaming and dwelling, where the animal either covers long distances or explores
256 locally, respectively [2,4]. The cGMP-dependent protein kinase EGL-4 acts in the sensory
257 neurons to promote dwelling [2]. *egl-4* loss of function mutant animals explore more than wild
258 type animals [2,4]. Also, *egl-4* mutations suppress the reduced exploration defect of *che-2*
259 mutants [2]. Thus, we examined whether *egl-4(n479)* mutant animals suppress the *grk-2*
260 exploration defect. We noticed that when the exploration assay was performed on 6 cm plates,
261 *egl-4* mutant animals didn't seem to explore significantly more than wild type animals, probably
262 due to a ceiling effect (Fig 4A). In contrast, when the assay was performed on 10 cm plates, *egl-*
263 *4* mutant animals explored significantly more than wild type animals (Fig 4B). In both cases, the
264 *egl-4(n479)* mutation significantly suppressed the *grk-2* exploration defect (Fig 4A,B).
265 Expression of EGL-4 in ciliated neurons reversed the *egl-4* suppression of the *grk-2* exploration
266 defect (Fig 4C), suggesting that GRK-2 and EGL-4 act in opposite ways in the ciliated neurons
267 to affect the exploration behavior.

268 EGL-4 also functions in sensory neurons to promote a *C. elegans* sleep state during
269 lethargus (lethargus quiescence; [3]). The described role of EGL-4 in quiescence prompted us
270 to examine whether the exploration defect of *grk-2* is the result of movement quiescence. We
271 measured activity and quiescence in *C. elegans* larval stage 4 (L4) animals by imaging
272 individual animals cultivated in a WorMotel, which is a micro-fabricated device with multiple

273 agar-filled wells [47,48]. Single L4 animals were placed in WorMotel, imaged for 8 h, and their
274 quiescence and activity were quantified. *grk-2(gk268)* mutant animals showed reduced body
275 movement activity and increased quiescence in this 8 h period and the *egl-4(n479)* mutation
276 suppressed these phenotypes (Fig 4D-F). We conclude that *grk-2* mutant animals have
277 enhanced movement quiescence that is suppressed by *egl-4*, indicating that *grk-2* and *egl-4* act
278 in opposite directions to regulate movement quiescence. These results also suggest that part of
279 the exploration defect of *grk-2* mutant might be the result of increased movement quiescence.
280 In addition to cGMP signaling through EGL-4, cAMP signaling pathways act through the
281 salt-inducible kinase KIN-29 in sensory neurons to regulate sensory behaviors [49]. *kin-29* plays
282 an important role in the metabolic regulation of sleep [50] and *kin-29* mutants, like *egl-4*
283 mutants, have reduced sleep. However, in contrast to *egl-4* mutant animals, *kin-29(oy38)*
284 mutant animals did not explore more than wild-type animals and the *kin-29(oy38)* mutation did
285 not rescue the exploration defect of *grk-2(gk268)* mutant (Fig S3B). We conclude that KIN-29
286 does not play a role in the GRK-2 pathway to control exploration and movement quiescence.
287
288 **APTF-1 promotes GRK-2-modulated movement quiescence and exploration**
289 To further explore the role of sleep in the reduced exploration of *grk-2* mutant, we
290 manipulated sleep in *grk-2* mutant animals. Sleep behavior is controlled by the AP2 transcription
291 factor APTF-1, which is required for the development of the sleep-promoting RIS interneuron
292 [51]. Although the exploration behavior of *aptf-1(gk794)* mutant animals was similar to that of
293 wild type animals, the *aptf-1* mutation partially suppressed the decreased exploration phenotype
294 of *grk-2* mutant animals (Fig 5A). Similarly, *aptf-1* mutant partially suppressed both the
295 enhanced quiescence and reduced activity phenotypes of *grk-2* mutant (Fig 5B-D). We
296 conclude that increased sleep is partially responsible for the reduced exploration phenotype of
297 *grk-2* mutant animals.

298 APTF-1 promotes sleep by turning on the expression of the sleep-inducing neuropeptide
299 FLP-11 in the RIS neuron. At sleep onset, increases in RIS calcium activity cause the release of
300 FLP-11, which induces quiescence [9]. *flp-11(tm2706)* mutant did not significantly affect the
301 exploration or quiescence phenotypes of *grk-2* mutant (Fig S4A-D), suggesting that GRK-2 acts
302 independently of FLP-11 in regulating quiescence, and that the role of APTF-1 in adult
303 movement quiescence is partially independent of FLP-11. Alternatively, since the effect of *flp-11*
304 on sleep is weaker than that of *aptf-1* [9], our assays might not be sensitive enough to detect a
305 phenotype for *flp-11*.
306 *C. elegans* displays an additional sleep-like quiescent behavior which occurs in
307 response to exposure to cellular stressors (stress-induced quiescence). Mutants lacking the
308 transcription factor CEH-17 lack a functional ALA neuron, a neuron which promotes stress-
309 induced quiescenc [13,14,52,53]. In contrast to the *aptf-1* mutation, the *ceh-17(np1)* mutation
310 did not affect the exploration or quiescence phenotypes of *grk-2* (Fig S4E-H), suggesting that
311 GRK-2 acts independently of the ALA neuron to control movement quiescence.
312
313 **NPR-1 negatively controls GRK-2- modulated exploration behavior**
314 The *C. elegans* neuropeptide receptor NPR-1 negatively regulates arousal by inhibiting
315 the activity of a sensory circuit that is connected by gap junctions to the RMG interneurons [54].
316 *npr-1* loss-of-function mutant animals have increased locomotion both in lethargus and in the
317 adult stage due to heightened activity of the RMG circuit [8,30-32,54]. *npr-1(ky13)* mutant
318 animals explored more than wild type animals and *npr-1(ky13)* suppressed the exploration
319 defect of *grk-2(gk268)* (Fig 6A,B). Moreover, *npr-1(ky13)* also suppressed the *grk-2* dispersal
320 defect in the absence of food (Fig 6C). These results suggest that *npr-1* and *grk-2* act in
321 opposite ways to affect the exploration behavior.
322 The FMRFamide-related neuropeptides (FaRPs) FLP-18 and FLP-21 are known NPR-1
323 ligands [55,56]. While *flp-18(db99)* and *flp-21(ok889)* single mutants did not have an exploration

324 defect, a *flp-18* mutation partially suppressed the defective exploration phenotype of *grk-2* (Fig
325 6D). The *flp-21* mutation did not affect the *grk-2* exploration defect and *flp-21; flp-18* mutants
326 were not stronger suppressors than *flp-18* mutants, suggesting that the *flp-21(ok889)* mutation
327 does not suppress the *grk-2* exploration defect (Fig 6E). The NPR-1 ligand FLP-18 only having
328 a partial effect suggests that it is not the only ligand for NPR-1 in this pathway. Alternatively,
329 NPR-1 may have ligand-independent activity.

330 NPR-1 is expressed in several neurons including neurons of the RMG circuit (ASH,
331 URX, RMG) [57] and expression in the RMG circuit completely rescues the increased
332 locomotion of *npr-1* mutants during lethargus [8,31]. Moreover, expression solely in the RMG
333 interneuron rescues the enhanced locomotion speed of *npr-1* mutants [54] while NPR-1 acts in
334 the ASH sensory neurons to inhibit sensory responses [8]. To examine whether ASH-specific
335 expression of *npr-1* is sufficient to reverse the *npr-1* suppression of the exploration defect of *grk-*
336 *2* mutants we expressed the *npr-1* cDNA under the control of the ASH (and ASI) - specific *sra-6*
337 promoter (*sra-6p*; [40]). Expression of *npr-1* under the *sra-6* promoter did not reverse the *npr-*
338 *1(ky13)* suppression of the exploration defect of *grk-2* (Fig 6F).

339 We next addressed whether RMG- specific expression of *npr-1* is sufficient to reverse
340 the *npr-1*- suppression of the exploration defect of *grk-2*. Since RMG- specific promoters are not
341 known, we used a described intersection strategy to drive *npr-1* expression only in the RMG
342 neuron [54]. In this approach, we used the *ncs-1* promoter to drive the Cre recombinase and the
343 *flp-21* promoter to drive *npr-1* preceded by a floxed STOP site. [54]. Expression of *npr-1* by this
344 method in *grk-2(gk268); npr-1(ky13)* mutant animals fully reversed the *npr-1* suppression of the
345 exploration defect of *grk-2* (Fig 6F). *flp-21* and *ncs-1* are coexpressed in several neurons
346 (including the RMG neurons), but of these neurons, *npr-1* is present only in ASE, ASG, and
347 RMG. Since ASE and ASG are gustatory neurons that have not been implicated in NPR-1
348 function in locomotion, our experiments suggest that NPR-1 functions in RMG to negatively
349 control the GRK-2 pathway that controls the exploration behavior.

350 **FLP-1 negatively controls GRK-2- mediated exploration behavior**

351 In a literature search for additional neuropeptides that could play a role in GRK-2-
352 modulated exploration, we came across FLP-1. *flp-1(ok2811)* null mutant animals are
353 hyperactive and have a loopy locomotion posture characterized by deep body bends [34-37].
354 Interestingly, although *flp-1(ok2811)* mutant animals explored as well as WT animals in the
355 presence of food, the *flp-1(ok2811)* mutation significantly suppressed the *grk-2(gk268)*
356 exploration defect (Fig 7A). Moreover, *grk-2(gk268); flp-1(ok2811); flp-18(db99)* triple mutant
357 animals behaved like the *grk-2(gk268); flp-1(ok2811)* double mutant, suggesting that FLP-1 and
358 FLP-18 act in the same pathway to negatively modulate GRK-2-mediated exploration behavior
359 (Fig 7B). Expression of FLP-1 under its own promoter and under the AVK neuron-specific *twk-*
360 *47* promoter reversed the *flp-1* suppression of the *grk-2* exploration phenotype, suggesting that
361 expression of FLP-1 in AVK interneurons is sufficient to restore its function (Fig 7C). To assess
362 whether *npr-1* and *flp-1* act in the same pathway, we built the triple mutant *grk-2; flp-1; npr-1*
363 and compared its phenotype with that of the *grk-2; npr-1* double mutant. We found that *grk-2;*
364 *flp-1; npr-1* behaves like *grk-2; npr-1* mutant animals, suggesting that either NPR-1 and FLP-1
365 act in the same pathway or that we cannot detect further suppression due to a ceiling effect (Fig
366 7D,E). Previous reports suggest that NPR-6 and FRPR-7 are low- and high-affinity FLP-1
367 receptors, respectively [36]. We tested the exploration behavior of *grk-2(gk268); npr-6(tm1497)*
368 and *grk-2(gk268); frpr-7(gk463846)* double mutants. *npr-6(tm1497)* did not affect the exploration
369 behavior of *grk-2(gk268),* but *frpr-7(gk463846)* partially but significantly suppressed the
370 exploration defect of *grk-2(gk268)* (Fig 7F). These results suggest that *frpr-7* but not *npr-6* could
371 be playing a role in the exploration behavior.

372

373 **GRK-2 negatively regulates FLP-1 secretion from the AVK neuron**

374 To examine the possibility of a functional connection between GRK-2 and FLP-1, we
375 assessed whether GRK-2 affects the levels of FLP-1 secretion using the coelomocyte uptake

assay [58-60]. Proteins that are secreted into the *C. elegans* body cavity are endocytosed by scavenger cells named coelomocytes (Fig 8A). We expressed the fusion protein FLP-1::mCherry in AVK neurons of *flp-1* single mutant animals and of *grk-2; flp-1* double mutant animals and quantified the intensity of fluorescence in coelomocytes as a readout of secreted FLP-1::mCherry (see Methods; [36]). Previous work confirmed that FLP-1::mCherry follows the dense core vesicle route for neuropeptide secretion and used the FLP-1::mCherry secretion assay as a way of evaluating FLP-1 secretion [36]. Notably, FLP-1::mCherry expression in *grk-2; flp-1* reversed the suppression of the exploration defect of *grk-2* by *flp-1,* suggesting that FLP-1 in the FLP-1::mCherry reporter retains its function in exploration (Fig S5). *grk-2; flp-1* mutants expressing FLP-1::mCherry had significantly increased levels of mCherry in coelomocytes in comparison to *flp-1* mutant animals (Fig 8A,B). To examine whether background fluorescence in the coelomocytes of *grk-2; flp-1* mutants also changed, together with FLP-1::mCherry we co-expressed a reporter expressing GFP driven by the coelomocyte-specific promoter *unc-122* and tested the levels of GFP fluorescence in the coelomocytes of *flp-1* and *grk-2; flp-1* mutants. We found that GFP fluorescence remained unchanged in *grk-2; flp-1* mutants suggesting that the increase in FLP-1::mCherry fluorescence in *grk-2; flp-1* coelomocytes is specific to FLP-1::mCherry (Fig 8C). These results suggest that GRK-2 affects the level of secreted FLP-1, which could explain at least in part the exploration defect observed in mutants lacking GRK-2. Consistent with this idea, multi-copy expression of FLP-1::mCherry under the *flp-1* promoter reduced the exploration behavior of wild type animals (Fig 8D). These results altogether indicate that GRK-2 negatively regulates the amount of FLP-1 that is secreted by AVK neurons, resulting in positive regulation of the exploration behavior.

398 ## Discussion

399 Locomotion is the result of dynamic interactions between a genetically determined
400 central program and feedback mechanisms that modulate the activity of the central program
401 [61]. Feedback is mainly of sensory and neuromodulatory nature and it plays a major role in
402 adapting the pattern of locomotion to environmental or metabolic changes [1]. Here we have
403 demonstrated that locomotor behavioral strategies in the nematode *Caenorhabditis elegans* are
404 altered through the action of the G protein-coupled receptor kinase-2 (GRK-2) in ciliated
405 sensory neurons and neuropeptide signaling in interneurons. We propose that GRK-2 acts in
406 ciliated sensory neurons to control the exploration behavior and the arousal state of the animal
407 by controlling the level of secretion of the neuropeptide FLP-1.
408

409 **GRK-2 signaling in ciliated sensory neurons controls exploration**

410 The sensory system influences the expression of different locomotor states in *C.*
411 *elegans*, like roaming and dwelling [2]. Roaming is a behavioral exploration strategy where the
412 animal covers long distances, while dwelling is a local search behavior strategy where animals
413 restrict their activity to a small region. Previous studies have shown that mutants with
414 diminished sensory responses to soluble and volatile chemicals are defective in the time they
415 spend roaming or dwelling, suggesting that sensory perception is critical for this behavior [2].
416 Specifically, a class of mutants that lack a normal sensory cilium structure, including *che-2*
417 [62,63], are unable to explore long distances. In this study we show that *grk-2* mutant animals
418 have similarly severe phenotypes as the cilium structure mutants in that they also show reduced
419 exploration. Our findings suggest that the positive role of GRK-2 in exploration behavior is due
420 to its positive role in chemosensation. We show that expression of GRK-2 in the ciliated sensory
421 neurons of *grk-2* mutant animals rescues their exploration defect, suggesting that GRK-2 acts
422 specifically in these neurons to affect exploration. Our effort to narrow down the specific
423 neurons where GRK-2 acts to mediate this behavior revealed that GRK-2 acts in multiple

424 ciliated neurons to control exploration. Interestingly, although *grk-2* mutant animals have strong
425 chemosensory defects, they do not have severe cilia structural defects like the cilium structure
426 mutants [23,64]. Also, expression of GRK-2 in adult *grk-2* mutant animals can rescue the *grk-2*
427 exploration defect suggesting that GRK-2 plays a non-developmental role in ciliated neurons to
428 promote exploration. Our study of mutants with defects in different kinds of sensory perception
429 showed that the activity of the ciliated neurons that are involved in chemosensation and
430 osmosensation play important roles in the exploration behavior, but neurons involved in
431 mechanosensation or oxygen-sensation do not. These results together suggest that impaired
432 sensory neuron function per se can reduce exploration.

433 Our results show that *grk-2* and the cilium structure mutant *che-2* act in the same
434 genetic pathway to control exploration, again suggesting that impaired ciliated sensory neuron
435 function disrupts exploration. In agreement, we found that mutations in the gene encoding the
436 cGMP-dependent protein kinase EGL-4 that suppress the altered exploration behavior of *che-2*
437 mutants [2], also suppress the exploration defect of *grk-2* mutant animals. Given that expression
438 of EGL-4 in the ciliated neurons reverses this suppression, we propose that both GRK-2 and
439 EGL-4 act in the same ciliated neurons to control exploration but in opposite ways. Given that
440 both GRK-2 and EGL-4 act in multiple ciliated neurons to control exploration behavior and that
441 other chemosensory and osmosensory mutants have similar exploration defects as *grk-2*, we
442 support a model in which GRK-2 acts in ciliated neurons to positively control sensory perception
443 and affect the exploration state of the animal by regulating EGL-4. We propose that in *grk-2* and
444 cilium structure mutants, impaired sensory perception leads to an increase in EGL-4 activity and
445 decreased exploration. A similar model was supported by previous studies, which showed that
446 EGL-4 in sensory neurons controls body size and locomotory states [2].

447 In previous work we have shown that GRK-2 regulates crawling and swimming [27,28]
448 by negatively regulating the D2-like dopamine receptor DOP-3 in premotor interneurons (Fig
449 9A). In the case of chemosensation and exploration, the target(s) of GRK-2, which are located

450 in chemosensory neurons and not interneurons, are currently unknown (Fig 9B). Similarly, we
451 do not yet know the identity of the phosphorylation target(s) for EGL-4.
452
453 **GRK-2 controls movement quiescence**
454 Animals undergo periods of quiescence and arousal in response to changes in their
455 environment or metabolic state. For example, *C. elegans* increases its exploration behavior
456 when it is removed from food [10,11] and shows quiescence during larval molting (lethargus)
457 and under starvation, satiety, and stress [3,12-17]. The cGMP-dependent protein kinase EGL-4
458 acts in sensory neurons to promote *C. elegans* sleep where the animals become quiescent
459 during lethargus [3]. This result, together with the observed opposite functionality between EGL-
460 4 and GRK-2 in ciliated neurons prompted us to examine whether *grk-2* mutants have
461 movement quiescence defects. Indeed, we found that *grk-2* mutant animals have enhanced
462 movement quiescence, which is suppressed by *egl-4*. This result suggests that GRK-2 and
463 EGL-4 act antagonistically to control movement quiescence outside lethargus. We propose that
464 GRK-2 acts in ciliated neurons to control sensory perception and affect movement quiescence
465 by negatively regulating EGL-4. Our findings imply that the exploration defect of *grk-2* and other
466 chemosensory mutants besides *grk-2* might be due in part to enhanced movement quiescence.
467 This series of data also suggests that *C. elegans* locomotion strategies that have been
468 described as exploration, roaming, and arousal might reflect the same behavior.
469 In addition to EGL-4, the AP2 transcription factor APTF-1 also plays an important role in
470 regulating sleep, largely by regulating expression of the sleep-inducing neuropeptide FLP-11 in
471 the RIS interneuron [51]. Indeed, we found that *aptf-1* mutants partially suppress the decreased
472 exploration phenotype, enhanced quiescence, and reduced activity of *grk-2*. This result
473 suggests that increased sleep is partially responsible for the reduced exploration phenotype of
474 *grk-2* mutant animals. Surprisingly, we found that *flp-11* mutations do not suppress the
475 enhanced quiescence of *grk-2* mutant animals. One possible explanation is that APTF-1 acts

476 through additional targets besides FLP-11, which is also supported by previous studies [9].
477 Alternatively, FLP-11 might be playing a smaller role than APTF-1 in adult quiescence and our
478 assays might not be sensitive enough to detect it.
479
480 **Neuromodulation through FLP-1 negatively regulates exploration**
481 Mutants lacking the neuropeptide receptor NPR-1 have been described as a model for
482 arousal both during lethargus and in adults [8,31-33]. NPR-1 is proposed to act in the RMG
483 interneuron to inhibit the activity of a sensory circuit that is connected to RMG via gap junctions
484 (54). In *npr-1* mutants, enhanced sensory activity causes aroused locomotion [8,31-33,65]. Our
485 results show that *npr-1* mutants suppress the exploration defects of *grk-2* mutant animals, and
486 that NPR-1 acts in RMG neurons to mediate this effect. The fact that *npr-1* is epistatic to *grk-2*
487 suggests that GRK-2 negatively regulates NPR-1 – in a *grk-2* mutant, increase in NPR-1 activity
488 inhibits exploration (Fig 9B). Since GRK-2 acts in ciliated neurons and NPR-1 acts in RMG
489 neurons to control exploration, this suggests that GRK-2 activity regulates NPR-1 in a cell-
490 nonautonomous way. Of the reported NPR-1 ligands FLP-18 and FLP-21, we found that only
491 FLP-18 acts in the GRK-2 pathway that mediates exploration, since *flp-18* mutants partially
492 suppress the exploration defect of *grk-2* [55,56]. Interestingly, we also found that mutants in the
493 gene encoding the neuropeptide FLP-1 partially suppress the *grk-2* exploration defect and that
494 FLP-1 acts in the same genetic pathway as FLP-18. FLP-1 has not been reported to be a
495 ligand for *C. elegans* NPR-1, but it was shown to activate the *Girardia tigrina* neuropeptide
496 receptor 1 GtNPR-1 when expressed in Chinese hamster ovary cells [66]. This finding together
497 with our genetic observations could suggest that FLP-1 directly acts through NPR-1 to affect
498 exploration. Alternatively, and since *flp-1* and *flp-18* mutants do not act in an additive way to
499 suppress the *grk-2* exploration defect, FLP-1 could be acting in the GRK-2 pathway through a
500 different receptor than NPR-1. The partial suppression of the *grk-2* exploration defect by *frpr-7*,
501 suggests that the high-affinity FLP-1 receptor FRPR-7 could be playing a role.

502 Notably, Oranth et al (2018) [36] suggested that after >10 min off food, AVK releases
503 FLP-1 peptides to promote dispersal. Our genetic experiments show that mutants in *flp-1*
504 suppress the exploration defect of *grk-2* mutant animals and that overexpression of FLP-1
505 reduces exploration in the presence of food. This apparent discrepancy might be attributed to
506 different FLP-1 functionality in the presence or absence of food or when chemosensation is
507 impaired. Our genetic results together with our finding that GRK-2 modulates the secretion
508 levels of FLP-1 suggest that GRK-2 negatively regulates FLP-1 secretion, either directly or
509 indirectly (Fig 9B). Since GRK-2 acts in ciliated neurons to affect exploration and GRK-2
510 modulates FLP-1 secretion from AVK neurons we propose that GRK-2 acts in ciliated neurons
511 to mediate FLP-1 secretion from AVKs in a cell-nonautonomous way. Given that there is no
512 known synaptic input from chemosensory neurons to AVKs [67] we suggest that GRK-2-driven
513 regulation of sensory neuron activity affects a neuromodulatory pathway that drives FLP-1
514 secretion from AVKs (Fig 9B). AVKs were previously reported to play important roles in
515 regulating locomotion by modulating motor neuron activity [36]. Alternatively, GRK-2 action in
516 ciliated neurons may lead to modulation of the neuronal circuit downstream of the ciliated
517 neurons that eventually affects secretion of FLP-1. According to our model, GRK-2 activity
518 positively regulates chemosensory neuron activity, which in turn inhibits EGL-4 activity,
519 modulating exploration and the arousal state of *C. elegans* through neuromodulatory signaling
520 acting in interneurons (Fig 9B). Thus, an active chemosensory system can guide *C. elegans*
521 towards exploration, while a defective chemosensory system inhibits dispersal and puts the
522 animal in a state of quiescence.

523 **Methods**

524 **Strains**

525 Strains were maintained at room temperature or 20° on the OP50 strain of *E. coli* [68].
526 The Supplementary Information contains a list of strains used, including their full genotypes
527 (Table S1; List of strains).

528

529 **Constructs and transgenes**

530 The Supplementary Information contains a list of constructs used (Table S2; List of
531 plasmids). All constructs made in this study were constructed using the Gateway system
532 (Invitrogen): a promoter region, a gene region (cDNA) or fluorescent tag, and a N- or C-terminal
533 3'UTR or fluorescent tag fused to a 3'UTR were cloned into the destination vector pCFJ150 [69].
534 For the cell-specific rescuing experiments, an operon GFP was included in the expression
535 constructs downstream of the 3'UTR [70]. This resulted in expression of untagged protein, but
536 also allowed for confirmation of proper promoter expression by monitoring GFP expression.
537 Extrachromosomal arrays were made by standard injection and transformation methods
538 [71]. We injected 5-10 ng/ul of the expression plasmid for *grk-2* and *flp-1* rescue experiments
539 and 20 ng/ul of the plasmids for other experiments. For the *yakEx261* FLP-1 overexpression
540 experiment in Fig 8D we injected 60 ng/ul. We injected 50 ng/ul of the *unc-122*::GFP co-
541 injection marker, 1 ng/ul of *myo-2p*::mCherry, 5 ng/ul of *myo-3p*::mCherry, and 5 ng/ul of *rab-*
542 *3p*::mCherry. We isolated two to three independent lines. The results shown in the figures are
543 for two of the lines tested.

544

545 **Exploration assays**

546 The exploration assay is an established assay that measures the ability of the animals to
547 explore (wander) during long periods of time [4]. Exploration assays were performed on 6 or 10
548 cm nematode growth medium (NGM) plates uniformly seeded with 200 or 500 ul of the OP50

549 strain of *E. coli*, respectively, and spread with a glass spreader. 10 cm plates were used in the
550 case of mutants that explore more than wild type animals (e.g. *egl-4, npr-1*) in order to avoid a
551 ceiling effect because wild type animals usually explore most of the area of a 6 cm plate in a
552 20h period. Bacteria were grown on the NGM agar surface at room temperature for
553 approximately 48 h and the plates were stored at 4°C until needed. On the day of the
554 experiment, individual first-day adult animals were transferred to the center of each plate and
555 were allowed to explore for 18-20 h. Then the plates were superimposed on a 50- or 150-
556 square grid and we counted the number of squares entered by the worm tracks. Approximately
557 10-40 animals were tested per strain. Every strain was tested in two or three independent trials.
558 The number "n" in figure legends indicates the total number of animals sampled (animals from
559 two or three different trials are combined).
560
561 **Dispersal assays**
562 The dispersal (or radial locomotion) assay is an established assay that measures the
563 distance animals travel from the middle of the plate in a period [38]. Since the dispersal assay
564 measures distance, it is only performed for short periods of time (1h on food or 20 min on plates
565 without food). Dispersal assays were performed on 10 cm nematode growth medium (NGM)
566 plates that were uniformly seeded with 500 µl of the OP50 strain of *E. coli* and spread with a
567 glass spreader. Bacteria were grown at room temperature for approximately 48 h and the plates
568 were stored at 4°C until needed. Approximately 20 first day adult animals were transferred to the
569 center of a plate and were allowed to explore for 1 h. Then the positions of the worms were
570 marked and the distances of the worms from the starting point were measured. Dispersal
571 assays without food were performed on NGM plates that were not spread with OP50 and the
572 animals were allowed to move freely for 20 min. Animals were first transferred to an
573 intermediate plate without food before being transferred to the assay plate. Approximately 20-60
574 animals were tested per strain. Every strain was tested in two or three independent trials. The

575 number “n” in figure legends indicates the total number of animals sampled (animals from two to
576 three different trials are combined).
577
578 **Heat shock assays**
579 Animals were raised to young adulthood at room temperature (23°C), then shifted to
580 34°C for 2 hr. They were allowed to recover at room temperature (23°C) for 4 hr and tested.
581
582 **Movement quiescence assays**
583 Movement quiescence assays were performed as previously described [48]. Briefly,
584 animals were selected as fourth larval stage L4s the day prior to the assay. They were loaded
585 individually onto the surface of NGM agar-filled wells on a PDMS WorMotel chip. The agar
586 surface in each well was covered in a thin lawn of DA837 *E. coli*. The loaded chip was placed in
587 a 10 cm petri dish lined with damp kimwipes to prevent desiccation and placed under a camera.
588 Images were acquired every 10 seconds for eight hours. The images were then analyzed using
589 a custom written program in Matlab. For more details on this method see [48]. 8-12 animals
590 were tested per condition and compared to 8-12 control animals imaged in the same WorMotel.
591 The “n” in figure legends indicates the total number of animals sampled.
592
593 **Body bend locomotion assays**
594 First-day adults were picked to a three-day-old lawn of OP50 and stimulated by poking
595 the tail of the animal with a worm pick. Body bends were then immediately counted for one
596 minute. A body bend was defined as the movement of the worm from maximum to minimum
597 amplitude of the sine wave. Approximately 10 animals were tested per strain. Every strain was
598 tested on two independent trials. The number “n” in figure legends indicates the total number of
599 animals sampled (animals from the different trials are combined).
600

601 **Imaging**

602 For fluorescence imaging, first-day adult animals were mounted on 2% agarose pads
603 and anesthetized with 50 mM sodium azide for ten minutes before placing the cover slip. The
604 animals were imaged using an Olympus FLUOVIEW FV1200 confocal microscope with a 60×
605 UPlanSApo oil objective (NA = 1.35) or a NikonTi2-E Crest X-light V2 spinning disk confocal
606 with a 60x oil objective (NA = 1.4).

607

608 **Coelomocyte assays**

609 For coelomocyte imaging we used FLP-1::mCherry (a gift from Alexander Gottschalk;
610 [36]). We imaged the anterior coelomocytes in day 1 adults using a NikonTi2-E Crest X-light V2
611 spinning disk confocal with a 60x oil 1.4 NA objective. Maximum intensity projections of image
612 stacks were obtained using FluoView software (Nikon). For quantification, the maximum
613 fluorescence intensity was calculated using Fiji and the background fluorescence intensity was
614 subtracted to obtain coelomocyte fluorescence.

615

616 **Statistics**

617 Statistical analysis and graphing were carried out using Prism 8 or Prism 9 (GraphPad
618 Software). Normally distributed data sets requiring multiple comparisons were analyzed by a
619 one-way ANOVA or by a one-way ANOVA followed by a Bonferroni test. Normally distributed
620 pairwise data comparisons were analyzed by two-tailed unpaired t tests. $p < 0.05$ (following
621 Bonferroni correction, when appropriate) was considered to be statistically significant (*$p < 0.05$,
622 **$p < 0.01$, ***$p < 0.001$, ****$p<0.0001$). Data are presented as the mean ± standard error
623 (SEM).

624 **Raw data**

625 Table S3 contains all the data points used for the main and supplementary figures.

## Acknowledgements

We dedicate this paper to the memory of Giannis Topalidis, whose support was instrumental for the completion of this manuscript. We thank Alexander Gottschalk for the FLP-1::mCherry plasmid, Ithai Rabinowitch for the *str-1, str-2,* and *odr-10* promoter plasmids, and Cori Bargmann for the pEM01 and pEM03 plasmids. Some strains were provided by the CGC, which is funded by the NIH Office of Research Infrastructure Programs (P40 OD010440). This work was funded by R01 NS109476 to MA and JB, R01 GM121481 to MA, R01 NS122779 and R01 NS107969 to DMR. KT was supported by a T32Act ES019851 Training grant (PI: Trever Penning).

## Author contributions

KD and IT conceived the experiments. KD and IT performed the experiments and analyzed the data. CM and OP performed the experiments described in Fig 3D. MA, DMR, and JB assisted with providing ideas. IT wrote the paper with help from MA, DMR, and JB.

641 **References**


642 1. MacKay-Lyons M. Central pattern generation of locomotion: a review of the evidence. Phys
643 Ther. 2002 Jan;82(1):69–83.

644 2. Fujiwara M, Sengupta P, McIntire SL. Regulation of body size and behavioral state of *C.*
645 *elegans* by sensory perception and the EGL-4 cGMP-dependent protein kinase. Neuron.
646 2002 Dec 19;36(6):1091–102.

647 3. Raizen DM, Zimmerman JE, Maycock MH, Ta UD, You Y jai, Sundaram MV, et al.
648 Lethargus is a *Caenorhabditis elegans* sleep-like state. Nature. 2008 Jan
649 31;451(7178):569–72.

650 4. Flavell SW, Pokala N, Macosko EZ, Albrecht DR, Larsch J, Bargmann CI. Serotonin and
651 the neuropeptide PDF initiate and extend opposing behavioral states in *C. elegans*. Cell.
652 2013 Aug 29;154(5):1023–35.

653 5. Flavell SW, Raizen DM, You YJ. Behavioral States. Genetics. 2020 Oct;216(2):315–32.

654 6. Flavell SW, Gordus A. Dynamic functional connectivity in the static connectome of
655 *Caenorhabditis elegans*. Curr Opin Neurobiol. 2022 Feb 17;73:102515.

656 7. Taghert PH, Nitabach MN. Peptide neuromodulation in invertebrate model systems.
657 Neuron. 2012 Oct 4;76(1):82–97.

658 8. Choi S, Taylor KP, Chatzigeorgiou M, Hu Z, Schafer WR, Kaplan JM. Sensory Neurons
659 Arouse *C. elegans* Locomotion via Both Glutamate and Neuropeptide Release. PLoS
660 Genet. 2015 Jul;11(7):e1005359.

661 9. Turek M, Besseling J, Spies JP, König S, Bringmann H. Sleep-active neuron specification
662 and sleep induction require FLP-11 neuropeptides to systemically induce sleep. eLife.
663 2016 Mar 7;5:e12499.

664 10. Gray JM, Hill JJ, Bargmann CI. A circuit for navigation in *Caenorhabditis elegans.* Proc
665 Natl Acad Sci U S A. 2005 Mar 1;102(9):3184–91.

666 11. Hills T, Brockie PJ, Maricq AV. Dopamine and glutamate control area-restricted search
667 behavior in *Caenorhabditis elegans.* J Neurosci. 2004 Feb 4;24(5):1217-25.

668 12. You Y jai, Kim J, Raizen DM, Avery L. Insulin, cGMP, and TGF-beta signals regulate food
669 intake and quiescence in *C. elegans*: a model for satiety. Cell Metab. 2008 Mar;7(3):249–
670 57.

671 13. Hill AJ, Mansfield R, Lopez JMNG, Raizen DM, Van Buskirk C. Cellular stress induces a
672 protective sleep-like state in *C. elegans*. Curr Biol CB. 2014 Oct 20;24(20):2399–405.

673 14. Nelson MD, Lee KH, Churgin MA, Hill AJ, Van Buskirk C, Fang-Yen C, et al. FMRFamide-
674 like FLP-13 neuropeptides promote quiescence following heat stress in *Caenorhabditis*
675 *elegans*. Curr Biol CB. 2014 Oct 20;24(20):2406–10.

676 15. DeBardeleben HK, Lopes LE, Nessel MP, Raizen DM. Stress-Induced Sleep After
677 Exposure to Ultraviolet Light Is Promoted by p53 in *Caenorhabditis elegans*. Genetics.
678 2017 Oct;207(2):571–82.

679 16. Skora S, Mende F, Zimmer M. Energy Scarcity Promotes a Brain-wide Sleep State
680 Modulated by Insulin Signaling in *C. elegans*. Cell Rep. 2018 Jan 23;22(4):953–66.

681 17. Wu Y, Masurat F, Preis J, Bringmann H. Sleep Counteracts Aging Phenotypes to Survive
682 Starvation-Induced Developmental Arrest in *C. elegans.* Curr Biol CB. 2018 Nov
683 19;28(22):3610-3624.e8.

684 18. Daniels SA, Ailion M, Thomas JH, Sengupta P. *egl-4* acts through a transforming growth
685 factor-beta/SMAD pathway in *Caenorhabditis elegans* to regulate multiple neuronal circuits
686 in response to sensory cues. Genetics. 2000 Sep;156(1):123–41.

687 19. L'Etoile ND, Coburn CM, Eastham J, Kistler A, Gallegos G, Bargmann CI. The cyclic GMP-
688 dependent protein kinase EGL-4 regulates olfactory adaptation in *C. elegans.* Neuron.
689 2002 Dec 19;36(6):1079–89.

690 20. McCloskey RJ, Fouad AD, Churgin MA, Fang-Yen C. Food responsiveness regulates
691 episodic behavioral states in *Caenorhabditis elegans.* J Neurophysiol. 2017 May
692 1;117(5):1911–34.

693 21. Gurevich VV, Gurevich EV. GPCR Signaling Regulation: The Role of GRKs and Arrestins.
694 Front Pharmacol. 2019;10:125.

695 22. Gurevich EV, Tesmer JJG, Mushegian A, Gurevich VV. G protein-coupled receptor
696 kinases: more than just kinases and not only for GPCRs. Pharmacol Ther. 2012
697 Jan;133(1):40–69.

698 23. Fukuto HS, Ferkey DM, Apicella AJ, Lans H, Sharmeen T, Chen W, et al. G protein-
699 coupled receptor kinase function is essential for chemosensation in *C. elegans.* Neuron.
700 2004 May 27;42(4):581–93.

701 24. Wood JF, Wang J, Benovic JL, Ferkey DM. Structural domains required for *Caenorhabditis*
702 *elegans* G protein-coupled receptor kinase 2 (GRK-2) function in vivo. J Biol Chem. 2012
703 Apr 13;287(16):12634–44.

704 25. Hukema RK, Rademakers S, Dekkers MPJ, Burghoorn J, Jansen G. Antagonistic sensory
705 cues generate gustatory plasticity in *Caenorhabditis elegans*. EMBO J. 2006 Jan
706 25;25(2):312–22.

707 26. Wang J, Luo J, Aryal DK, Wetsel WC, Nass R, Benovic JL. G protein-coupled receptor
708 kinase-2 (GRK-2) regulates serotonin metabolism through the monoamine oxidase AMX-2
709 in *Caenorhabditis elegans.* J Biol Chem. 2017 Apr 7;292(14):5943–56.

710 27. Topalidou I, Cooper K, Pereira L, Ailion M. Dopamine negatively modulates the NCA ion
711 channels in *C. elegans*. PLoS Genet. 2017 Oct;13(10):e1007032.

712 28. Xu Y, Zhang L, Liu Y, Topalidou I, Hassinan C, Ailion M, et al. Dopamine receptor DOP-1
713 engages a sleep pathway to modulate swimming in *C. elegans.* iScience. 2021 Apr
714 23;24(4):102247.

715 29. Heilman C, Ibarreta J, Salonga GA, Hon MC, Caracci AM, Badial T, et al. G protein
716 coupled receptor kinases modulate *Caenorhabditis elegans* reactions to heat stresses.
717 Biochem Biophys Res Commun. 2020 Oct 1;530(4):692–8.

718 30. Henry SA, Crivello S, Nguyen TM, Cybulska M, Hoang NS, Nguyen M, et al. G protein-
719 coupled receptor kinase 2 modifies the ability of *Caenorhabditis elegans* to survive
720 oxidative stress. Cell Stress Chaperones. 2021 Jan;26(1):187–97.

721 31. Choi S, Chatzigeorgiou M, Taylor KP, Schafer WR, Kaplan JM. Analysis of NPR-1 reveals
722 a circuit mechanism for behavioral quiescence in *C. elegans*. Neuron. 2013 Jun
723 5;78(5):869–80.

724 32. Nichols ALA, Eichler T, Latham R, Zimmer M. A global brain state underlies *C. elegans*
725 sleep behavior. Science. 2017 Jun 23;356(6344):eaam6851.

726 33. Soto R, Goetting DL, Van Buskirk C. NPR-1 Modulates Plasticity in *C. elegans* Stress-
727 Induced Sleep. iScience. 2019 Sep 27;19:1037–47.

728 34. Hums I, Riedl J, Mende F, Kato S, Kaplan HS, Latham R, et al. Regulation of two motor
729 patterns enables the gradual adjustment of locomotion strategy in *Caenorhabditis elegans.*
730 eLife. 2016 May 25;5:e14116.

731 35. Buntschuh I, Raps DA, Joseph I, Reid C, Chait A, Totanes R, et al. FLP-1 neuropeptides
732 modulate sensory and motor circuits in the nematode *Caenorhabditis elegans.* PloS One.
733 2018;13(1):e0189320.

734 36. Oranth A, Schultheis C, Tolstenkov O, Erbguth K, Nagpal J, Hain D, et al. Food Sensation
735 Modulates Locomotion by Dopamine and Neuropeptide Signaling in a Distributed Neuronal
736 Network. Neuron. 2018 Dec 19;100(6):1414-1428.e10.

737 37. Topalidou I. Background mutation in strain RB2126 affects the locomotion behavior of *flp-1*
738 mutants. MicroPublication Biol. 2021 May 9;2021.

739 38. Coleman B, Topalidou I, Ailion M. Modulation of Gq-Rho Signaling by the ERK MAPK
740 Pathway Controls Locomotion in *Caenorhabditis elegans.* Genetics. 2018 Jun;209(2):523–
741 35.

742 39. Roayaie K, Crump JG, Sagasti A, Bargmann CI. The G alpha protein ODR-3 mediates
743 olfactory and nociceptive function and controls cilium morphogenesis in *C. elegans*
744 olfactory neurons. Neuron. 1998 Jan;20(1):55–67.

745 40. Troemel ER, Chou JH, Dwyer ND, Colbert HA, Bargmann CI. Divergent seven
746 transmembrane receptors are candidate chemosensory receptors in *C. elegans.* Cell. 1995
747 Oct 20;83(2):207–18.

748 41. Sengupta P, Chou JH, Bargmann CI. *odr-10* encodes a seven transmembrane domain
749 olfactory receptor required for responses to the odorant diacetyl. Cell. 1996 Mar
750 22;84(6):899–909.

751 42. Troemel ER, Kimmel BE, Bargmann CI. Reprogramming chemotaxis responses: sensory
752 neurons define olfactory preferences in *C. elegans.* Cell. 1997 Oct 17;91(2):161–9.

753 43. Troemel ER, Sagasti A, Bargmann CI. Lateral signaling mediated by axon contact and
754 calcium entry regulates asymmetric odorant receptor expression in *C. elegans.* Cell. 1999
755 Nov 12;99(4):387–98.

756 44. Yu S, Avery L, Baude E, Garbers DL. Guanylyl Cyclase expression in specific sensory
757 neurons: a new family of chemosensory receptors. Proc Natl Acad Sci U S A. 1997 Apr
758 1;94(7):3384–7.

759 45. Flames N, Hobert O. Gene regulatory logic of dopamine neuron differentiation. Nature.
760 2009 Apr 1;458(7240):885–9.

761 46. Inglis PN, Ou G, Leroux MR, Scholey JM. The sensory cilia of *Caenorhabditis elegans.*
762 2007 Mar 8; WormBook, ed. The *C. elegans* Research Community, WormBook. Available
763 from: http://www.wormbook.org

764 47. Churgin MA, Jung SK, Yu CC, Chen X, Raizen DM, Fang-Yen C. Longitudinal imaging of
765 *Caenorhabditis elegans* in a microfabricated device reveals variation in behavioral decline
766 during aging. eLife. 2017 May 31;6:e26652.

767 48. Churgin MA, Szuperak M, Davis KC, Raizen DM, Fang-Yen C, Kayser MS. Quantitative
768 imaging of sleep behavior in *Caenorhabditis elegans* and larval Drosophila melanogaster.
769 Nat Protoc. 2019 May;14(5):1455–88.

770 49. van der Linden AM, Wiener S, You Y jai, Kim K, Avery L, Sengupta P. The EGL-4 PKG
771 acts with KIN-29 salt-inducible kinase and protein kinase A to regulate chemoreceptor
772 gene expression and sensory behaviors in *Caenorhabditis elegans.* Genetics. 2008
773 Nov;180(3):1475–91.

774 50. Grubbs JJ, Lopes LE, van der Linden AM, Raizen DM. A salt-induced kinase is required for
775 the metabolic regulation of sleep. PLoS Biol. 2020 Apr;18(4):e3000220.

776 51. Turek M, Lewandrowski I, Bringmann H. An AP2 transcription factor is required for a sleep-
777 active neuron to induce sleep-like quiescence in *C. elegans.* Curr Biol CB. 2013 Nov
778 18;23(22):2215–23.

779 52. Pujol N, Torregrossa P, Ewbank JJ, Brunet JF. The homeodomain protein
780 CePHOX2/CEH-17 controls antero-posterior axonal growth in *C. elegans.* Dev Camb Engl.
781 2000 Aug;127(15):3361–71.

782 53. Trojanowski NF, Nelson MD, Flavell SW, Fang-Yen C, Raizen DM. Distinct Mechanisms
783 Underlie Quiescence during Two *Caenorhabditis elegans* Sleep-Like States. J Neurosci
784 Off J Soc Neurosci. 2015 Oct 28;35(43):14571–84.

785 54. Macosko EZ, Pokala N, Feinberg EH, Chalasani SH, Butcher RA, Clardy J, et al. A hub-
786 and-spoke circuit drives pheromone attraction and social behaviour in *C. elegans.* Nature.
787 2009 Apr 30;458(7242):1171–5.

788 55. Kubiak TM, Larsen MJ, Nulf SC, Zantello MR, Burton KJ, Bowman JW, et al. Differential
789 activation of "social" and "solitary" variants of the *Caenorhabditis elegans* G protein-
790 coupled receptor NPR-1 by its cognate ligand AF9. J Biol Chem. 2003 Sep
791 5;278(36):33724–9.

792 56. Rogers C, Reale V, Kim K, Chatwin H, Li C, Evans P, et al. Inhibition of *Caenorhabditis*
793 *elegans* social feeding by FMRFamide-related peptide activation of NPR-1. Nat Neurosci.
794 2003 Nov;6(11):1178–85.

795 57. Coates JC, de Bono M. Antagonistic pathways in neurons exposed to body fluid regulate
796 social feeding in *Caenorhabditis elegans*. Nature. 2002 Oct 31;419(6910):925–9.

797 58. Fares H, Greenwald I. Genetic analysis of endocytosis in *Caenorhabditis elegans:*
798 coelomocyte uptake defective mutants. Genetics. 2001 Sep;159(1):133–45.

799 59. Sieburth D, Madison JM, Kaplan JM. PKC-1 regulates secretion of neuropeptides. Nat
800 Neurosci. 2007 Jan;10(1):49–57.

801 60. Speese S, Petrie M, Schuske K, Ailion M, Ann K, Iwasaki K, et al. UNC-31 (CAPS) Is
802 Required for Dense-Core Vesicle But Not Synaptic Vesicle Exocytosis in *Caenorhabditis*
803 *elegans.* J Neurosci. 2007 Jun 6;27(23):6150–62.

804 61. Rossignol S, Dubuc R, Gossard JP. Dynamic sensorimotor interactions in locomotion.
805 Physiol Rev. 2006 Jan;86(1):89–154.

806 62. Lewis JA, Hodgkin JA. Specific neuroanatomical changes in chemosensory mutants of the
807 nematode *Caenorhabditis elegans.* J Comp Neurol. 1977 Apr 1;172(3):489–510.

808 63. Perkins LA, Hedgecock EM, Thomson JN, Culotti JG. Mutant sensory cilia in the nematode
809 *Caenorhabditis elegans.* Dev Biol. 1986 Oct;117(2):456–87.

810 64. Mukhopadhyay S, Lu Y, Shaham S, Sengupta P. Sensory signaling-dependent remodeling
811 of olfactory cilia architecture in *C. elegans.* Dev Cell. 2008 May;14(5):762–74.

812 65. Nagy S, Tramm N, Sanders J, Iwanir S, Shirley IA, Levine E, et al. Homeostasis in *C.*
813 *elegans* sleep is characterized by two behaviorally and genetically distinct mechanisms.
814 eLife. 2014 Dec 4;3:e04380.

815 66. Omar HH, Humphries JE, Larsen MJ, Kubiak TM, Geary TG, Maule AG, et al. Identification
816 of a platyhelminth neuropeptide receptor. Int J Parasitol. 2007 Jun;37(7):725–33.

817 67. White JG, Southgate E, Thomson JN, Brenner S. The structure of the nervous system of
818 the nematode *Caenorhabditis elegans.* Philos Trans R Soc Lond B Biol Sci. 1986 Nov
819 12;314(1165):1–340.

820 68. Brenner S. The genetics of *Caenorhabditis elegans.* Genetics. 1974 May;77(1):71–94.

821 69. Frøkjær-Jensen C, Davis MW, Sarov M, Taylor J, Flibotte S, LaBella M, et al. Random and
822 targeted transgene insertion in *Caenorhabditis elegans* using a modified Mos1 transposon.
823 Nat Methods. 2014 May;11(5):529–34.

824 70. Frøkjær-Jensen C, Davis MW, Ailion M, Jorgensen EM. Improved Mos1-mediated
825 transgenesis in *C. elegans.* Nat Methods. 2012 Jan 30;9(2):117–8.

826 71. Mello CC, Kramer JM, Stinchcomb D, Ambros V. Efficient gene transfer in *C.elegans*:
827 extrachromosomal maintenance and integration of transforming sequences. EMBO J. 1991
828 Dec;10(12):3959–70.

829

830

831 **Figure captions**

832 **Fig 1. *grk-2* mutant animals have dispersal and exploration defects.**

833 (A) Schematic representation of the assay used to measure dispersal (see Methods).

834 (B) *grk-2(gk268)* mutant animals have a dispersal defect in the presence of food and *dop-*

835 *3(vs106)* does not rescue this phenotype. Shown is the distance (cm) animals traveled from the

836 center of the plate in the presence of food in 1 h. (****, P<0.0001. ns, P>0.05. One way ANOVA

837 followed by a Bonferroni test. Error bars = SEM; n = 30–53).

838 (C) *grk-2(gk268)* mutant animals have a dispersal defect in the absence of food and *dop-*

839 *3(vs106)* does not rescue this phenotype. Shown is the distance (cm) animals traveled from the

840 center of the plate without food in 20 min. (****, P<0.0001. ns, P>0.05. One way ANOVA

841 followed by a Bonferroni test. Error bars = SEM; n = 47-60).

842 (D) Schematic representation of the assay used to measure exploration (see Methods).

843 (E) *grk-2(gk268)* mutant hermaphrodites have an exploration defect and *dop-3(vs106)* does not

844 rescue this defect. Shown is the number of squares (out of 50) single animals covered in

845 approximately 20 h. (****, P<0.0001. ns, P>0.05. One way ANOVA followed by a Bonferroni

846 test. Error bars = SEM; n = 30-32).

847 (F) *grk-2(gk268)* mutant males have an exploration defect. (****, P<0.0001. Student's t-test.

848 Error bars = SEM; n = 30).

849

850 **Fig 2. *grk-2* acts in the ciliated neurons to control exploration behavior.**

851 (A) Expression of *grk-2* cDNA under a pan-neuronal promoter rescues the exploration defect of

852 *grk-2* mutant animals in the presence of food. The *grk-2* cDNA was expressed in *grk-2(gk268)*

853 mutant animals under a pan-neuronal promoter (*rab-3p*, transgene *yakEx44*), ventral cord

854 acetylcholine motor neuron promoter (*acr-2p*, transgene *yakEx47*), and interneuron promoter

855 (*nmr-1p*, transgene *yakSi32*). Shown is the number of squares single animals covered in ~20 h.

856 (****, P<0.0001. ns, P>0.05. One way ANOVA followed by a Bonferroni test. Error bars = SEM;
857 n = 20-25).
858 (B) Expression of *grk-2* cDNA under either of two ciliated sensory neuron promoters (*xbx-1p*,
859 transgene *yakEx71* and *osm-6p*, transgene *yakEx53*) rescues the exploration defect of *grk-*
860 *2(gk268)* mutant animals in the presence of food. (****, P<0.001. ns, P>0.05. One way ANOVA
861 followed by a Bonferroni test. Error bars = SEM; n = 20-30).
862 (C) Expression of *grk-2* cDNA under a ciliated sensory neuron promoter (*xbx-1p::grk-2*,
863 transgene *yakEx71*) rescues the dispersal defect of *grk-2(gk268)* in the absence of food. (****,
864 P<0.0001. ns, P>0.05. One way ANOVA followed by a Bonferroni test. Error bars = SEM; n =
865 49-55). Please note the high variability in the off-food response in comparison to the on-food
866 response (Fig. 2B). This could be because worms are more mobile in the absence of food and
867 constantly searching for a food source, which would increase the variability of the distances they
868 cover.
869 (D) Expression of *grk-2* cDNA under the *odr-3* promoter (expression in AWA, AWB, AWC, ASH,
870 and ADF neurons; *odr-3p::grk-2*, transgene *yakEx189*) partially rescues the exploration defect
871 of *grk-2(gk268)*. (****, P<0.0001. One way ANOVA followed by a Bonferroni test. Error bars =
872 SEM; n = 27-44).
873 (E) Expression of *grk-2* cDNA under the *sra-6* promoter (expression in ASH and ASI neurons;
874 *sra-6p::grk-2*, transgene *yakEx191*) or under the combined control of the *odr-10* (AWA
875 neurons), *str-1* (AWB neurons) and *str-2* (AWC ON neuron) promoters (*str-1p, str-2p, odr-*
876 *10p::grk-2*, transgene *yakEx194*) partially rescues the exploration defect of *grk-2(gk268)*. (****,
877 P<0.0001. One way ANOVA followed by a Bonferroni test. Error bars = SEM; n = 25-44).
878 (F) Expression of *grk-2* cDNA under the *odr-10p* (AWA), *str-1p* (AWB), or *str-2p* (AWC ON)
879 promoters (transgenes *pekEx267, pekEx265* and *pekEx266,* respectively) partially rescues the
880 *grk-2* exploration defect. (***, P<0.001. **, P<0.01. *, P<0.05. One way ANOVA followed by a

881 Bonferroni test. Error bars = SEM; n = 20-33). Twenty of the data points shown for WT and *grk-*
882 *2* mutant are the same as in Figure 3B (these experiments were run in parallel).
883 (G) *grk-2* is expressed in many neurons in the head of the worm including *odr-3*- expressing
884 neurons. Representative images of the z-stack projections of the head of an animal co-
885 expressing tagRFP fused to GRK-2 ORF driven by the *grk-2* promoter (*grk-2*::tagRFP,
886 transgene *yakIs19*) and NLS-tagged mNeon driven by the *odr-3* promoter (*odr-3p*::mNeon::NLS;
887 transgene *yakEx204*). Arrows indicate *grk-2*::tagRFP-expressing cells that also express *odr-*
888 *3p*::mNeon::NLS. Scale bar: 10 μm.
889 (H) Expression of *grk-2* cDNA under the *gcy-8* promoter (expression in AFD neurons; *gcy-*
890 *8p::grk-2*, transgene *yakEx202*) fails to rescue the exploration defect of *grk-2(gk268)*.
891 (ns, P>0.05. One way ANOVA followed by a Bonferroni test. Error bars = SEM; n = 20-40).
892 (I) Expression of *grk-2* cDNA under the *dat-1* promoter (expression in dopaminergic neurons;
893 *dat-1p::grk-2*, transgene *yakEx259*) fails to rescue the exploration defect of *grk-2(gk268)*. (ns,
894 P>0.05. Student's t-test. Error bars = SEM; n = 38-44).
895 (J) Expression of *grk-2* cDNA under the heat shock promoter *hsp-16.41* (*hsp-16.41p::grk-2*,
896 transgene *yakEx253*) in adult *grk-2(gk268)* partially but significantly rescues their exploration
897 defect. (****, P<0.0001. Student's t-test. Error bars = SEM; n = 34-44).
898
899 **Fig 3. Mutants in cilia-related genes have exploration defects.**
900 (A) The *che-2(e1033)* mutant has an exploration defect like *grk-2(gk268)* that is not enhanced
901 by *grk-2*. Shown is the number of squares single animals covered in ~20 h. (****, P<0.0001. ns,
902 P>0.05. One way ANOVA followed by a Bonferroni test. Error bars = SEM; n = 22).
903 (B) The *daf-10(e1387)* mutant has an exploration defect like *grk-2(gk268)* that is not enhanced
904 by *grk-2*. Shown is the number of squares single animals covered in ~20 h. (****, P<0.0001. ns,
905 P>0.05. One way ANOVA followed by a Bonferroni test. Error bars = SEM; n = 20-25). The data

906 points shown for WT and *grk-2* mutant are the same as in Figure 2F (these experiments were
907 run in parallel).
908 (C) The *che-2(e1033)* and *daf-10(e1387)* mutants have a dispersal defect independently of food
909 that is not enhanced by *grk-2(gk268).* Shown is the distance (cm) animals traveled from the
910 center of the plate without food in 20 min. (****, P<0.0001. One way ANOVA followed by a
911 Bonferroni test. Error bars = SEM; n = 30-40).
912 (D) Most chemosensory and osmosensory-defective mutants that possess strong or weak
913 cilium-structure defects based on a dye-filling assay ([46]; shown in blue and green,
914 respectively) have exploration defects. Chemosensory-defective mutants *odr-1, odr-3, odr-8,*
915 *odr-10, tax-2,* and *tax-4*; osmosensory-defective mutants *osm-7* and *osm-10;* and
916 thermosensory-defective mutant *ttx-1(p767),* also have exploration defects. In contrast,
917 chemosensory mutants *che-1, che-6, che-7, odr-2, odr-4, odr-5, odr-7,* osmosensory mutants
918 *osm-9* and *osm-11*, oxygen-sensing mutant *gcy-35,* and mechanosensory-defective mutants
919 *mec-3, mec-4,* and *glr-1* do not have exploration defects. The canonical null allele *ocr-2(ak47)*
920 (strain VM396; indicated with an asterisk) showed a significant exploration defect that was not
921 observed with the presumably null allele *ocr-2(ok1711)*. Outcrossed strain BJH2763 *ocr-2(ak47)*
922 did not show a similar exploration defect, suggesting that the *ocr-2(ak47)* mutation per se does
923 not cause exploration defects (Fig S3A; see text for details). Shown is the number of squares
924 (out of 50) single animals covered in ~20 h, normalized to WT. (***, P<0.001. **, P<0.01. *,
925 P<0.05. ns, P>0.05. One way ANOVA followed by a Bonferroni test. Error bars = SEM; n = 10-
926 35).
927
928 **Fig 4. *egl-4* suppresses the exploration defect, movement quiescence, and reduced**
929 **activity of *grk-2* mutant animals.**
930 (A), (B) The *egl-4(n479)* mutation partially suppresses the exploration defect of *grk-2(gk268)*
931 mutant as assayed on 6 cm (A) and 10 cm (B) plates. Shown is the number of squares (out of

932 50, (A) or 150, (B)) single animals covered in ~20 h. Please note that *egl-4* mutant animals
933 explore more than wild type animals as assayed on 10 cm plates. (****, P<0.0001. ns, P>0.05.
934 One way ANOVA followed by a Bonferroni test. Error bars = SEM; n = 22-26).
935 (C) Expression of *egl-4* cDNA in ciliated sensory neurons under the *osm-6* promoter reverses
936 the *egl-4* suppression of the exploration defect of *grk-2* mutant (*osm-6p::egl-4*, transgene
937 *yakEx221*). Shown is the number of squares single animals covered in ~20 h (****, P<0.0001.
938 ns, P>0.05. Student's t-test. Error bars = SEM; n = 31-33).
939 (D) *grk-2(gk268)* mutant animals show enhanced movement quiescence, and the *egl-4(n479)*
940 mutation suppresses this phenotype. The graph shows the average minutes animals spent in
941 quiescence per hour in the WorMotel. Quiescence is the time when zero worm pixels moved
942 between two frames separated by 10 sec (See Methods). One WT animal was considered an
943 outlier and was not included in the graph since its values were more than 3 standard deviations
944 from the mean.
945 (E) The graph shows the total minutes individual animals spent in quiescence in 8 h in the
946 WorMotel. (****, P<0.0001. ns, P>0.05. One way ANOVA. Error bars = SEM; n = 11-12).
947 (F) *grk-2(gk268)* mutant animals show reduced activity, and the *egl-4(n479)* mutation partially
948 suppresses this phenotype. The graph shows the activity in pixels of individual animals in 8 h in
949 the WorMotel. Activity is the number of pixels moved between frames separated by 10 sec.
950 (****, P<0.0001. One way ANOVA. Error bars = SEM; n = 11-12).
951
952 **Fig 5. *aptf-1* partially suppresses the exploration defect, movement quiescence, and**
953 **reduced activity of *grk-2*.**
954 (A) The *aptf-1(gk794)* mutation partially suppresses the exploration defect of *grk-2(gk268)*
955 mutant. Shown is the number of squares single animals covered in ~20 h. (****, P<0.0001. ns,
956 P>0.05. One way ANOVA followed by a Bonferroni test. Error bars = SEM; n = 21-62).

957 (B) *grk-2(gk268)* mutant animals show enhanced movement quiescence, and the *aptf-1(gk794)*
958 mutation partially suppresses this phenotype. The graph shows the average minutes animals
959 spent in quiescence per hour in the WorMotel. Quiescence is the time when zero pixels moved
960 between two frames separated by 10 sec (See Methods).
961 (C) *grk-2(gk268)* mutant animals show enhanced movement quiescence, and the *aptf-1(gk794)*
962 mutation partially suppresses this phenotype. The graph shows the total minutes individual
963 animals spent in quiescence in 8 h in the WorMotel. (****, P<0.0001. ns, P>0.05. One way
964 ANOVA. Error bars = SEM; n = 10-12).
965 (D) *grk-2(gk268)* mutant animals show reduced activity, and the *aptf-1(gk794)* mutation partially
966 suppresses this phenotype. The graph shows the activity in pixels of individual animals in 8 h in
967 the WorMotel. Activity is the number of pixels moved between frames separated by 10 sec.
968 (****, P<0.05. **, P<0.01. One way ANOVA. Error bars = SEM; n = 10-12).
969
970 **Fig 6. *npr-1* suppresses the exploration defect of *grk-2* mutant animals.**
971 (A) The *npr-1(ky13)* mutation suppresses the exploration defect of *grk-2(gk268)* mutants as
972 assayed on 6 cm plates. Shown is the number of squares (out of 50) single animals covered in
973 ~20 h. (****, P<0.0001. *, P<0.05. ns, P>0.05. One way ANOVA followed by a Bonferroni test.
974 Error bars = SEM; n = 20-42).
975 (B) The *npr-1(ky13)* mutation suppresses the exploration defect of *grk-2(gk268)* mutant as
976 assayed on 10 cm plates. Shown is the number of squares (out of 150) single animals covered
977 in ~20 h. (****, P<0.0001. *, P<0.05. One way ANOVA followed by a Bonferroni test. Error bars
978 = SEM; n = 23-25).
979 (C) The *npr-1(ky13)* mutation suppresses the dispersal defect of *grk-2(gk268)* in the absence of
980 food. (****, P<0.0001. ***, P<0.001. ns, P>0.05. One way ANOVA followed by a Bonferroni
981 test. Error bars = SEM; n = 39-51).

982 (D) The *flp-18(db99)* mutation partially but significantly suppresses the exploration defect of *grk-*
983 *2(gk268)*. (****, P<0.0001. ns, P>0.05. One way ANOVA followed by a Bonferroni test. Error
984 bars = SEM; n = 20-30). The data points shown for WT and *grk-2* mutant are the same as in
985 Figure S4A (these experiments were run in parallel).
986
987 (E) The *flp-21(ok889)* mutation does not suppress the exploration defect of *grk-2(gk268)*. (****,
988 P<0.0001. **, P<0.01. ns, P>0.05. One way ANOVA followed by a Bonferroni test. Error bars =
989 SEM; n = 20-26).
990 (F) Expression of *ncs-1p::nCre* and *flp-21p*::LoxStopLox::NPR-1 (expression in RMG neurons
991 ((54); *RMGp::npr-1*, transgene *yakEx206*) reverses the *npr-1* suppression of the exploration
992 defect of *grk-2(gk268)* mutant. Expression of *npr-1* cDNA under the *sra-6* promoter (expression
993 in ASH and ASI neurons; *sra-6p::npr-1*, transgene *yakEx209*) fails to reverse the *npr-1*
994 suppression of the exploration defect of *grk-2(gk268)* (****, P<0.0001. ns, P>0.05. One way
995 ANOVA followed by a Bonferroni test. Error bars = SEM; n = 21-33).
996
997 **Fig 7. *flp-1* significantly suppresses the exploration defect of *grk-2*.**
998 (A) *grk-2(gk268)* mutant animals have an exploration defect and *flp-1(ok2811)* significantly
999 suppresses this defect. Shown is the number of squares (out of 50) single animals covered in
1000 ~20 h. (****, P<0.0001. One way ANOVA followed by a Bonferroni test. Error bars = SEM; n =
1001 20-26).
1002 (B) *flp-1* and *flp-18* act in the same pathway to regulate exploration. *flp-1(ok2811)* and *flp-*
1003 *18(db99)* partially suppress the exploration defect of *grk-2(gk268)* mutant and the *grk-2(gk268);*
1004 *flp-1(ok2811); flp-18(db99)* triple mutant behaves like the *grk-2(gk268); flp-1(ok2811)* double
1005 mutant. (****, P<0.0001. ***, P<0.001. ns, P>0.05. One way ANOVA followed by a Bonferroni
1006 test. Error bars = SEM; n = 20-28).

1007 (C) Expression of *flp-1* under its own promoter (*flp-1p::flp-1*, transgene *yakEx231*) or under the
1008 *twk-47* promoter (expression in AVK neurons; *twk-47p::flp-1*, transgene *yakEx216),* reverses the
1009 *flp-1* suppression of the exploration defect of *grk-2(gk268)* mutant. (****, P<0.0001. Student's t-
1010 test. Error bars = SEM; n = 23-30).
1011 (D) *npr-1(ky13)* suppresses the dispersal defect of *grk-2(gk268)* mutant and the *grk-2(gk268);*
1012 *flp-1(ok2811); npr-1(ky13)* triple mutant behaves like the *grk-2(gk268); npr-1(ky13)* double
1013 mutant. Shown is the distance (cm) animals traveled from the center of the plate in the presence
1014 of food in 1 h. (ns, P>0.05. One way ANOVA followed by a Bonferroni test. Error bars = SEM; n
1015 = 51-67).
1016 (E) *npr-1(ky13)* suppresses the exploration defect of *grk-2(gk268)* mutant and the *grk-2(gk268);*
1017 *flp-1(ok2811); npr-1(ky13)* triple mutant behaves like the *grk-2(gk268); npr-1(ky13)* double
1018 mutant. Shown is the number of squares (out of 50) single animals covered in ~20 h (ns,
1019 P>0.05. One way ANOVA followed by a Bonferroni test. Error bars = SEM; n = 20-23).
1020 (F) *frpr-7(gk463846)* partially but significantly suppresses the exploration defect of *grk-2(gk268)*
1021 mutant. *npr-6(tm1497)* has no effect on *grk-2(gk268)* exploration. (***, P<0.001. ns, P>0.05.
1022 One way ANOVA followed by a Bonferroni test. Error bars = SEM; n = 23-39).

1023 **Fig 8. *grk-2* mutant animals expressing FLP-1::mCherry show increased fluorescence in**
1024 **their coelomocytes.**
1025 (A) (Up) Schematic diagram of the coelomocyte uptake assay used to quantify FLP-1 secretion
1026 from AVK interneurons. (Down) Representative images of coelomocytes of *flp-1(ok2811)* and
1027 *grk-2(gk268); flp-1(ok2811)* mutant animals expressing a rescuing construct of FLP-1::mCherry
1028 (FLP-1::mCherry; transgene *yakEx256*). Scale bars = 10 μm.
1029 (B) mCherry fluorescence intensity of coelomocytes of *flp-1(ok2811)* and *grk-2(gk268); flp-*
1030 *1(ok2811)* mutant animals expressing FLP-1::mCherry and a coelomocyte marker *unc-*

1031 *122*::GFP. (FLP-1::mCherry; transgene *yakEx256).* (**, P<0.01. Student's t-test. Error bars =
1032 SEM; n = 57-59).
1033 (C) GFP fluorescence intensity of coelomocytes of *flp-1(ok2811)* and *grk-2(gk268); flp-*
1034 *1(ok2811)* mutant animals expressing FLP-1::mCherry and a coelomocyte marker *unc-*
1035 *122*::GFP (*unc-122::GFP*; transgene *yakEx256*). (ns, P>0.05. Student's t-test. Error bars =
1036 SEM; n = 29-30).
1037 (D) Overexpression of FLP-1 reduces the exploration behavior of wild type animals. Shown is
1038 the number of squares covered in ~20 h by single wild type animals, *flp-1* mutant expressing
1039 low levels of FLP-1::mCherry (transgene *yakEx256;* 5 ng/ul injected), and wild type animals
1040 overexpressing FLP-1 (transgene *yakEx261;* 60 ng/ul injected). (****, P<0.0001. ***, P<0.001.
1041 One way ANOVA followed by a Bonferroni test. Error bars = SEM; n = 29-47).
1042
1043 **Fig 9. Model for GRK-2 modulation of locomotion behaviors in *C. elegans.***
1044 GRK-2 positively controls (A) crawling and swimming by acting in premotor interneurons in a
1045 manner that depends on the D2-like dopamine receptor DOP-3 [27,28] and (B) exploration by
1046 acting in ciliated neurons in an opposite way from EGL-4. We propose a model in which GRK-2
1047 acts in multiple ciliated sensory neurons to positively control sensory perception and (1) inhibit
1048 the activity of the EGL-4 kinase in the same ciliated neurons, (2) negatively regulate the
1049 neuropeptide receptor NPR-1 in RMG interneurons in a cell-nonautonomous way (e.g. by
1050 regulating the level of secretion of an NPR-1 ligand), and (3) negatively control the levels of
1051 FLP-1 secretion from AVK interneurons. AVKs play critical roles in regulating locomotion by
1052 modulating motor neuron activity [36]. Since the ciliated neurons and AVK interneurons do not
1053 have direct connections, we propose that GRK-2 controls FLP-1 secretion from AVK
1054 interneurons in a cell-nonautonomous way through a neuromodulatory pathway. Proteins that
1055 positively regulate crawling, swimming, or exploration are shown in green and proteins that

1056 negatively regulate crawling, swimming, or exploration are shown in red. Dashed lines show
1057 indirect interactions. Created with BioRender.com.
1058
1059 **Fig S1. *grk-2* acts in parallel to *pdfr-1* and *tph-1* to control exploration.**
1060 (A) *grk-2(gk268)* and *pdfr-1(ok3425)* mutants have exploration defects. The double mutant *grk-*
1061 *2(gk268); pdfr-1(ok3425)* has a stronger phenotype than the single mutants suggesting that
1062 these genes act in parallel to control exploration behavior. Shown is the number of squares (out
1063 of 50) single animals covered in ~20 h. (****, P<0.0001. **, P<0.01. One way ANOVA followed
1064 by a Bonferroni test. Error bars = SEM; n = 23-28).
1065 (B) *grk-2(gk268)* mutant animals explore less and *tph-1(mg280)* more than WT animals. The
1066 double mutant *tph-1(mg280); grk-2(gk268)* has an intermediate phenotype suggesting that
1067 these genes act in parallel pathways to control exploration behavior. (****, P<0.0001. ***,
1068 P<0.001. One way ANOVA followed by a Bonferroni test. Error bars = SEM; n = 23-41).
1069
1070 **Fig S2. *grk-2* acts in command interneurons to regulate crawling.**
1071 *grk-2* cDNA expression in command interneurons (*Pnmr-1*, transgene *yakSi32*) is sufficient to
1072 rescue the slow locomotion of *grk-2(gk268)* mutant animals. (****, P<0.0001. ns, P>0.05. One
1073 way ANOVA followed by a Bonferroni test. Error bars = SEM; n = 20).
1074
1075 **Fig S3. *ocr-2(ak47), ocr-2(ok1711,)* and *kin-29(oy38)* mutants do not have exploration**
1076 **defects.**
1077 (A) *ocr-2(ak47), ocr-2(ok1717)* (strains BJH2763 and BJH2762, respectively) and *kin-29(oy38)*
1078 mutants do not have exploration defects. Shown is the number of squares (out of 50) single
1079 animals covered in ~20 h. (ns, P>0.05. One way ANOVA followed by a Bonferroni test. Error
1080 bars = SEM; n = 20-24).

1081 (B) *kin-29(oy38)* mutant animals do not have an exploration defect and the double mutant *grk-*
1082 *2(gk268); kin-29(oy38*) has an exploration defect similar to *grk-2(gk268).* (ns, P>0.05. One way
1083 ANOVA followed by a Bonferroni test. Error bars = SEM; n = 20-21).
1084
1085 **Fig S4. Mutations in *flp-11* and *ceh-17* do not affect the exploration defect and movement**
1086 **quiescence of *grk-2*.**
1087 (A) The *flp-11(tm2706)* mutation does not affect the exploration defect of *grk-2(gk268)* mutant
1088 animals. Shown is the number of squares (out of 50) single animals covered in ~20 h. (****,
1089 P<0.0001. ns, P>0.05. One way ANOVA followed by a Bonferroni test. Error bars = SEM; n =
1090 20-28). The data points shown for WT and *grk-2* mutant are the same as in Figure 6D (these
1091 experiments were run in parallel).
1092 (B) *grk-2(gk268)* mutant animals show enhanced movement quiescence and the *flp-11(tm2706)*
1093 mutation does not affect this phenotype. The graph shows the average minutes animals spent in
1094 quiescence per hour in the WorMotel. Quiescence is the time when there
1095 were zero pixels moved between two frames separated by 10 sec (See Methods).
1096 (C) The graph shows the total minutes individual animals spent in quiescence in 8h in the
1097 WorMotel. (****, P<0.0001. ns, P>0.05. One way ANOVA. Error bars = SEM; n = 11-12).
1098 (D) *grk-2(gk268)* mutant animals show reduced activity and the *flp-11(tm2706)* mutation does
1099 not affect this phenotype. The graph shows the activity in pixels of individual animals in 8 h in
1100 the WorMotel. Activity is the number of pixels moved between frames separated by 10 sec.
1101 (****, P<0.0001. ns, P>0.05. One way ANOVA. Error bars = SEM; n = 11-12).
1102 (E) The *ceh-17(np1)* mutation does not affect the exploration defect of *grk-2(gk268)* mutant
1103 animals. Shown is the number of squares (out of 50) single animals covered in ~20 h. (ns,
1104 P>0.05. One way ANOVA. Error bars = SEM; n = 20-24).
1105 (F) *grk-2(gk268)* mutant animals show enhanced movement quiescence, and the *ceh-17(np1)*
1106 mutation does not affect this phenotype.

1107 (G) The graph shows the total minutes individual animals spent in quiescence in 8 h in the
1108 WorMotel. (*, P<0.05. ***, P<0.001. ns, P>0.05. One way ANOVA. Error bars = SEM; n = 8-12).
1109 (H) The graph shows the activity in pixels of individual animals in 8 h in the WorMotel.
1110 (****, P<0.0001. ns, P>0.05. Error bars = SEM; n = 8-12).
1111
1112 **Fig S5. Expression of FLP-1::mCherry in *grk-2; flp-1* mutant animals reverses the**
1113 **suppression of the *grk-2* exploration defect by *flp-1*.**
1114 Shown is the number of squares (out of 50) single animals covered in ~20 h. (****, P<0.0001.
1115 ns, P>0.05. One way ANOVA followed by a Bonferroni test. Error bars = SEM; n = 34-39).
1116
1117 **Table S1. List of strains.**
1118 **Table S2. List of plasmids.**
1119 **Table S3. Raw data.**
1120

**Figure 1**

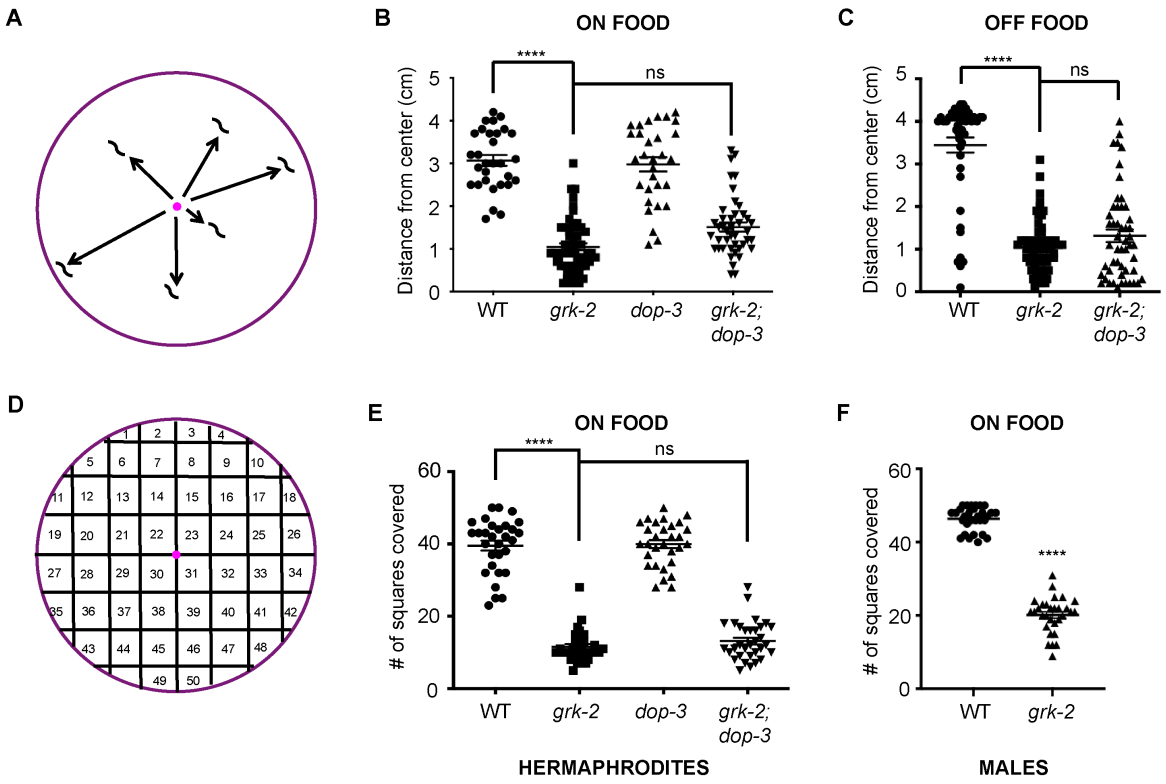
A
B
ON FOOD
Distance from center (cm)
****
ns
WT
grk-2
dop-3
grk-2; dop-3
C
OFF FOOD
D
E
ON FOOD
# of squares covered
HERMAPHRODITES
F
ON FOOD
MALES

## Figure 2

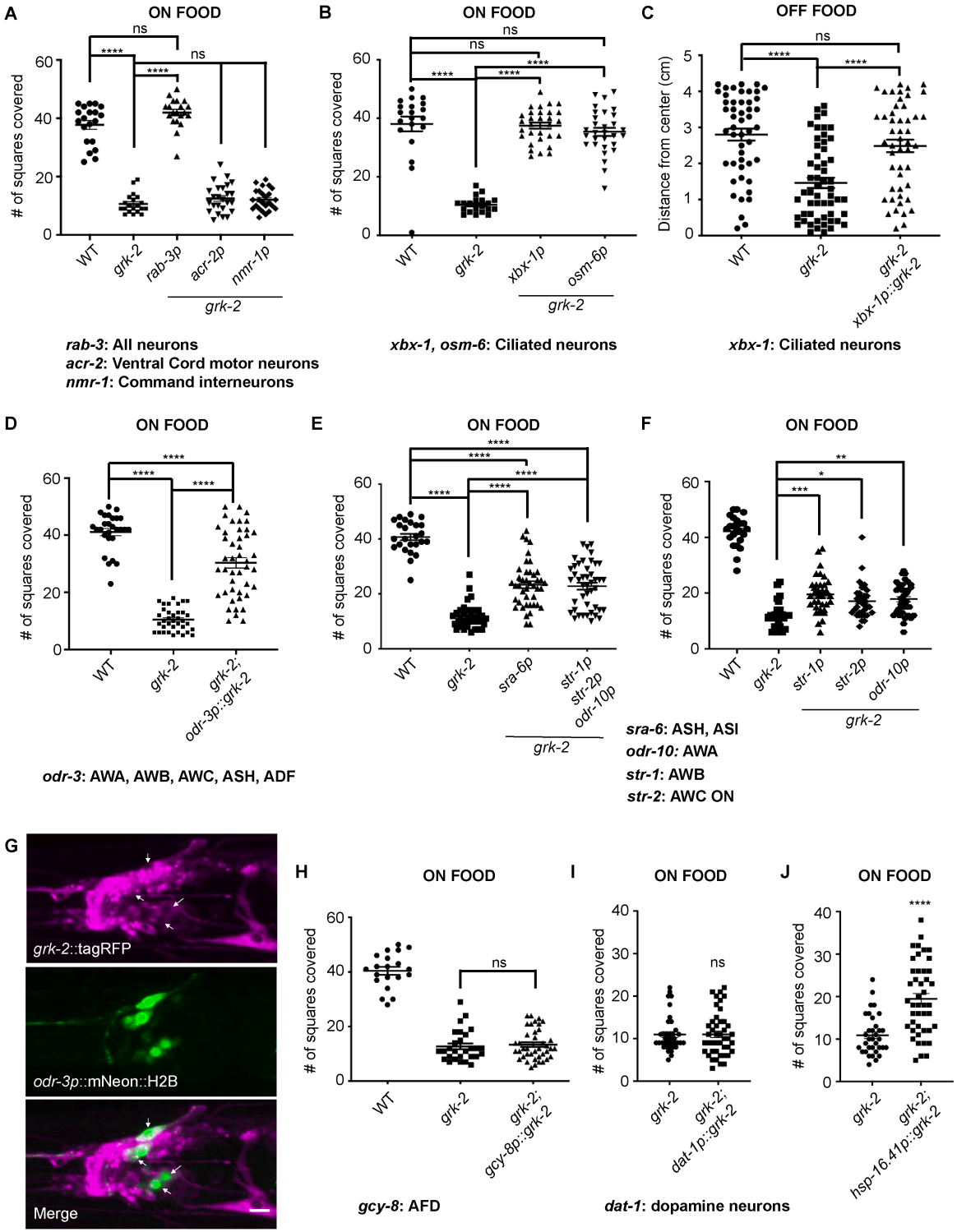
A
ON FOOD
# of squares covered
WT
grk-2
rab-3p
acr-2p
nmr-1p
grk-2
ns
****
B
ON FOOD
# of squares covered
WT
grk-2
xbx-1p
osm-6p
grk-2
C
OFF FOOD
Distance from center (cm)
WT
grk-2
grk-2 xbx-1p::grk-2
rab-3: All neurons
acr-2: Ventral Cord motor neurons
nmr-1: Command interneurons
xbx-1, osm-6: Ciliated neurons
xbx-1: Ciliated neurons
D
ON FOOD
# of squares covered
WT
grk-2
grk-2; odr-3p::grk-2
odr-3: AWA, AWB, AWC, ASH, ADF
E
ON FOOD
# of squares covered
WT
grk-2
sra-6p
str-1p
str-2p
odr-10p
grk-2
F
ON FOOD
# of squares covered
WT
grk-2
str-1p
str-2p
odr-10p
grk-2
**
*
***
sra-6: ASH, ASI
odr-10: AWA
str-1: AWB
str-2: AWC ON
G
grk-2::tagRFP
odr-3p::mNeon::H2B
Merge
H
ON FOOD
# of squares covered
WT
grk-2
grk-2; gcy-8p::grk-2
gcy-8: AFD
I
ON FOOD
# of squares covered
grk-2
grk-2; dat-1p::grk-2
dat-1: dopamine neurons
J
ON FOOD
# of squares covered
grk-2
grk-2; hsp-16.41p::grk-2

## Figure 3

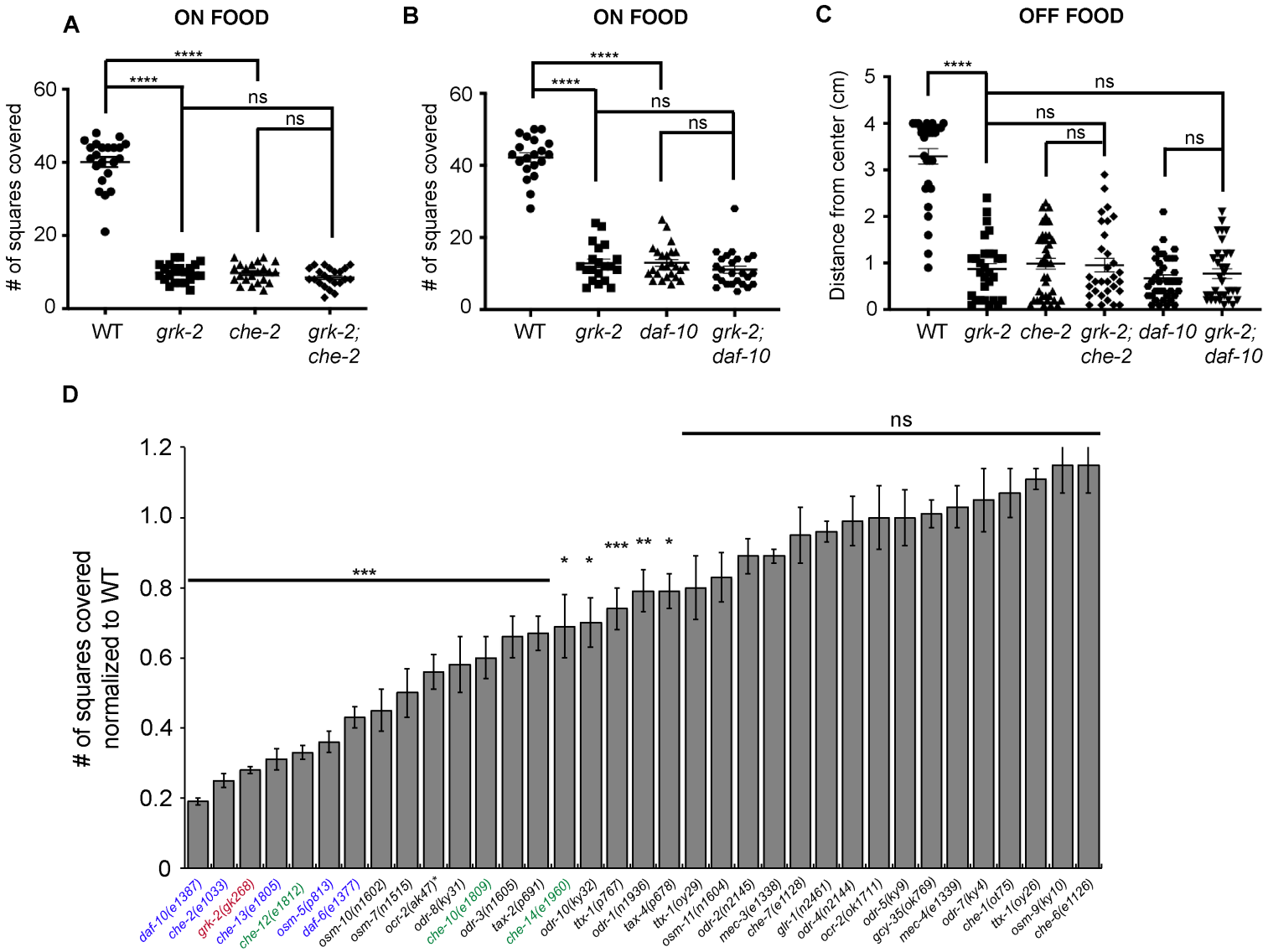
A
ON FOOD
# of squares covered
WT
grk-2
che-2
grk-2; che-2
B
ON FOOD
# of squares covered
WT
grk-2
daf-10
grk-2; daf-10
C
OFF FOOD
Distance from center (cm)
WT
grk-2
che-2
grk-2; che-2
daf-10
grk-2; daf-10
D
# of squares covered normalized to WT
daf-10(e1387)
che-2(e1033)
grk-2(gk268)
che-13(e1805)
che-12(e1812)
osm-5(p813)
daf-6(e1377)
osm-10(n1602)
osm-7(n1515)
ocr-2(ak47)*
odr-8(ky31)
che-10(e1809)
odr-3(n1605)
tax-2(p691)
che-14(e1960)
odr-10(ky32)
ttx-1(p767)
odr-1(n1936)
tax-4(p678)
ttx-1(oy29)
osm-11(n1604)
odr-2(n2145)
mec-3(e1338)
che-7(e1128)
glr-1(n2461)
odr-4(n2144)
ocr-2(ok1711)
odr-5(ky9)
gcy-35(ok769)
mec-4(e1339)
odr-7(ky4)
che-1(ot75)
ttx-1(oy26)
osm-9(ky10)
che-6(e1126)

## Figure 4

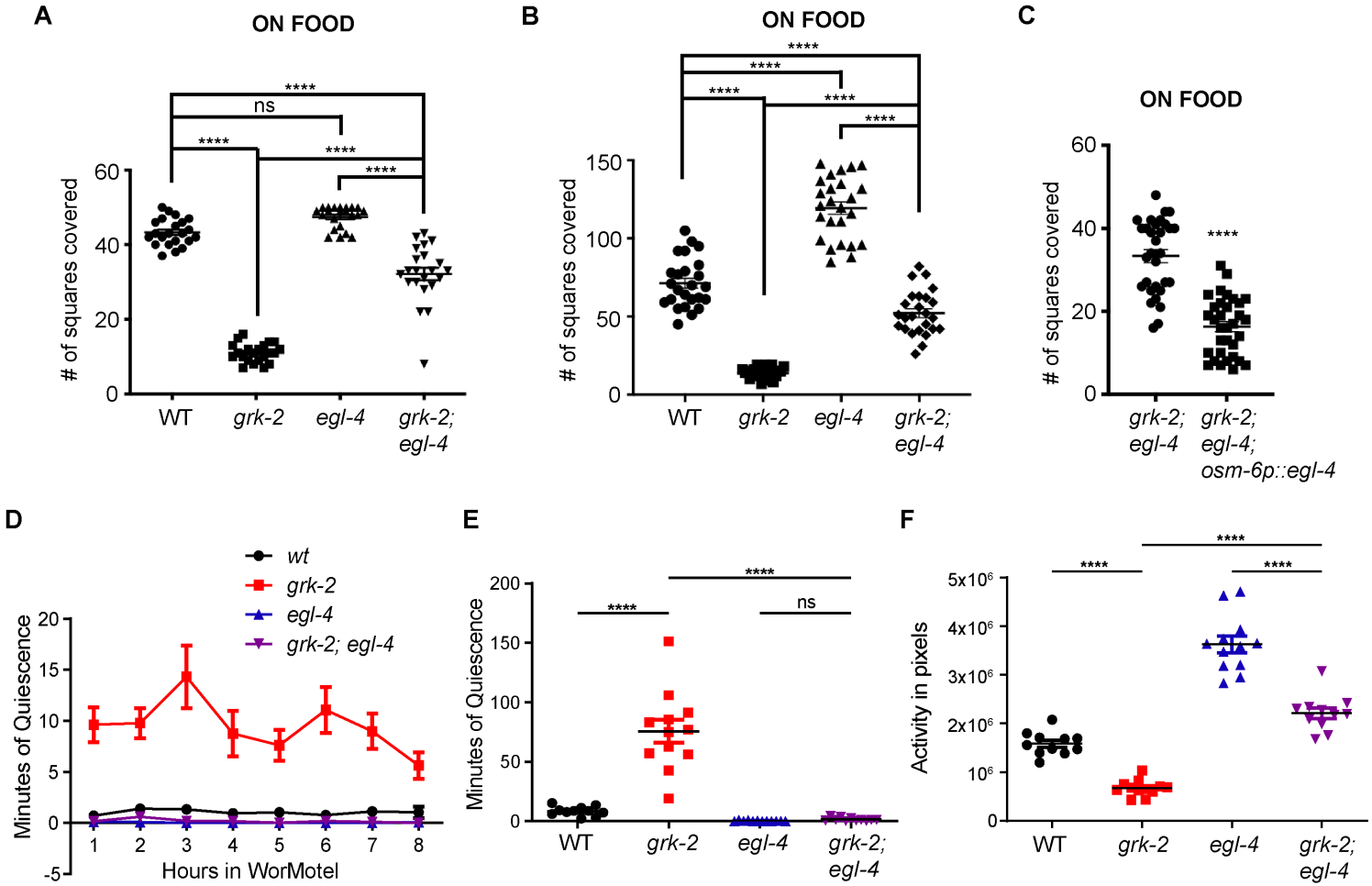
A
ON FOOD
# of squares covered
WT
grk-2
egl-4
grk-2; egl-4
****
ns
B
ON FOOD
# of squares covered
C
ON FOOD
# of squares covered
grk-2; egl-4
grk-2; egl-4; osm-6p::egl-4
D
wt
grk-2
egl-4
grk-2; egl-4
Minutes of Quiescence
Hours in WorMotel
E
Minutes of Quiescence
F
Activity in pixels

## Figure 5

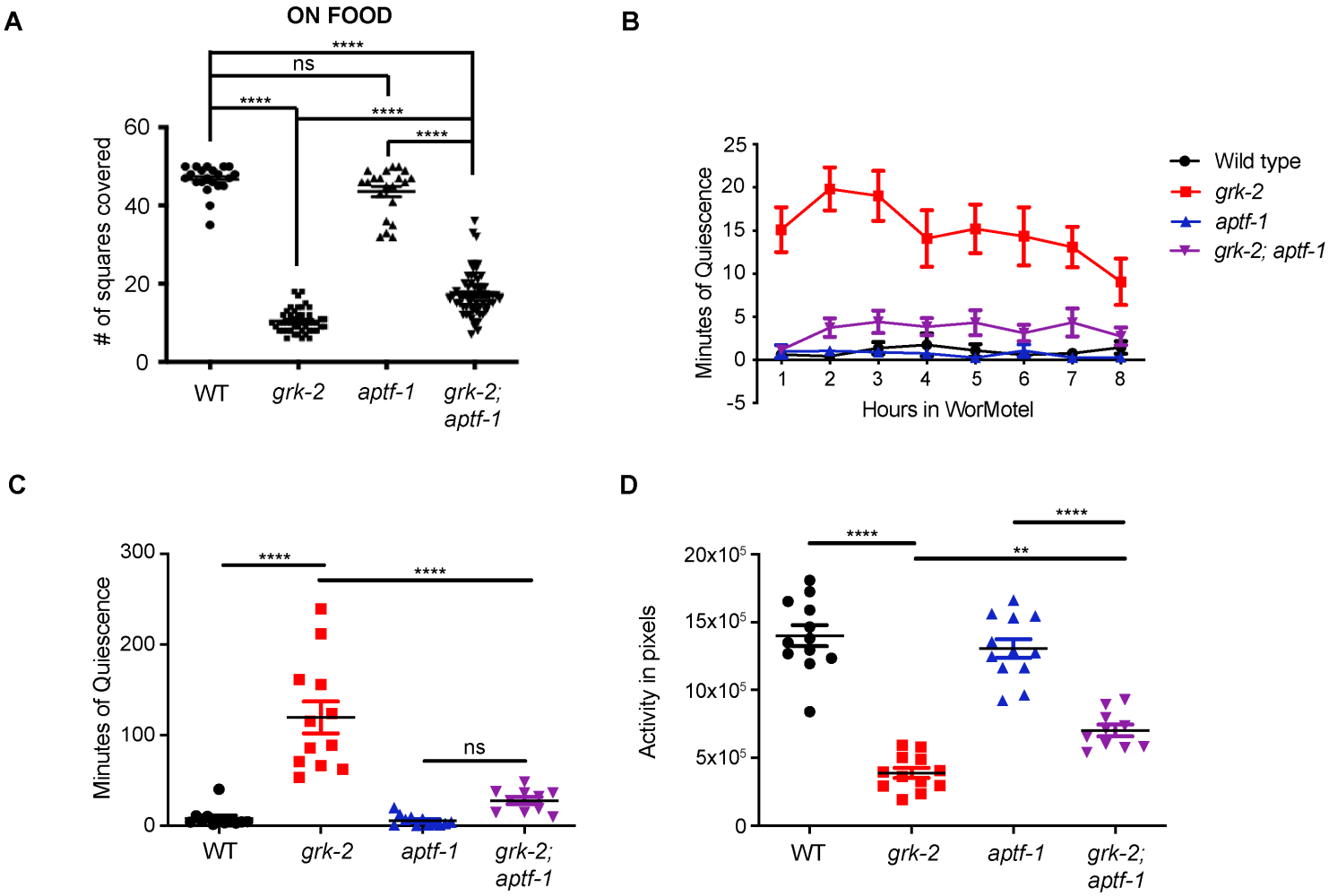
A
ON FOOD
****
ns
****
****
****
# of squares covered
60
40
20
0
WT
grk-2
aptf-1
grk-2; aptf-1
B
Minutes of Quiescence
25
20
15
10
5
0
-5
1
2
3
4
5
6
7
8
Hours in WorMotel
Wild type
grk-2
aptf-1
grk-2; aptf-1
C
Minutes of Quiescence
300
200
100
0
****
****
ns
WT
grk-2
aptf-1
grk-2; aptf-1
D
Activity in pixels
20x10^5
15x10^5
10x10^5
5x10^5
0
****
**
****
WT
grk-2
aptf-1
grk-2; aptf-1

**Figure 6**

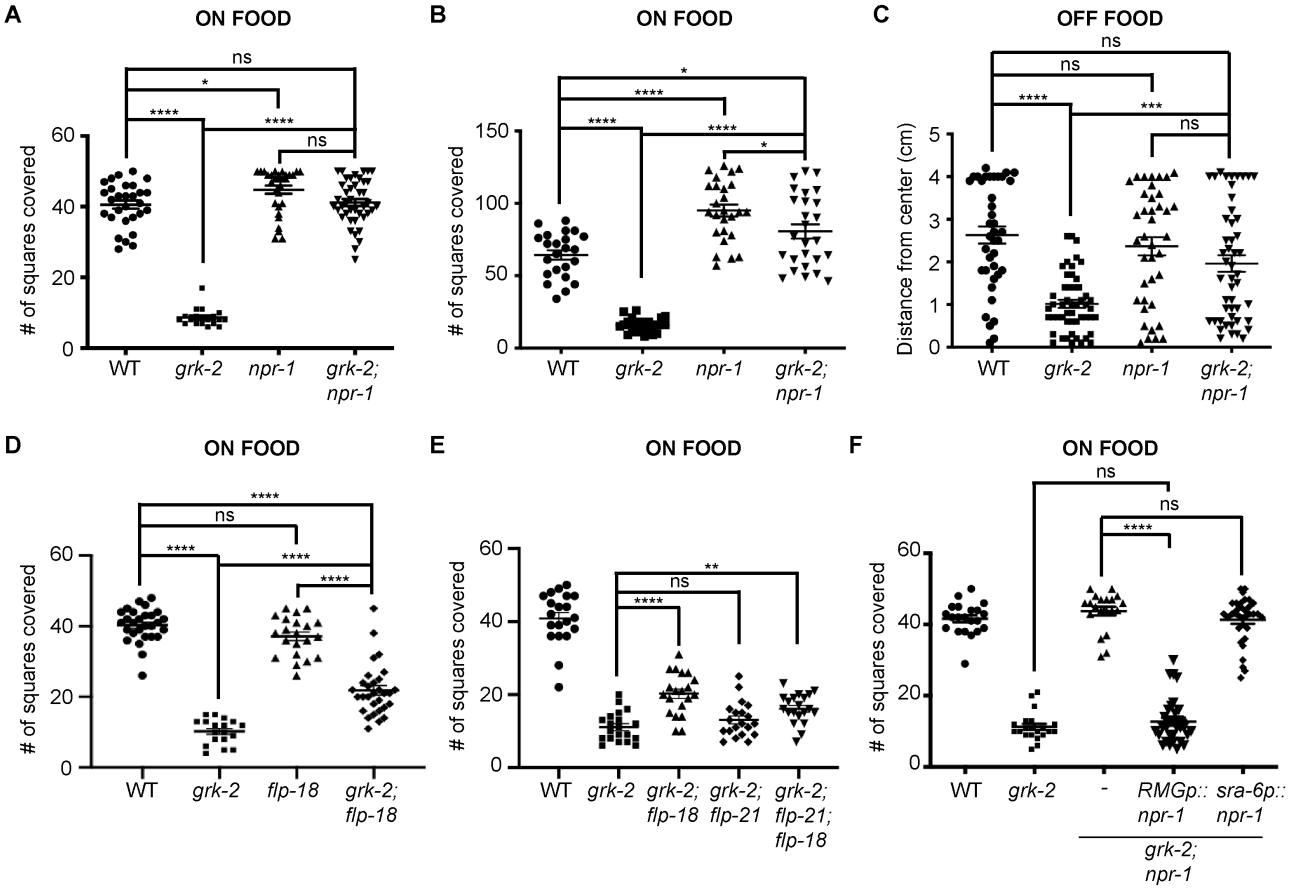
A
ON FOOD
# of squares covered
WT
grk-2
npr-1
grk-2; npr-1
B
ON FOOD
# of squares covered
C
OFF FOOD
Distance from center (cm)
D
ON FOOD
# of squares covered
WT
grk-2
flp-18
grk-2; flp-18
E
ON FOOD
# of squares covered
grk-2; flp-18
grk-2; flp-21
grk-2; flp-21; flp-18
F
ON FOOD
# of squares covered
-
RMGp:: npr-1
sra-6p:: npr-1
grk-2; npr-1

**Figure 7**

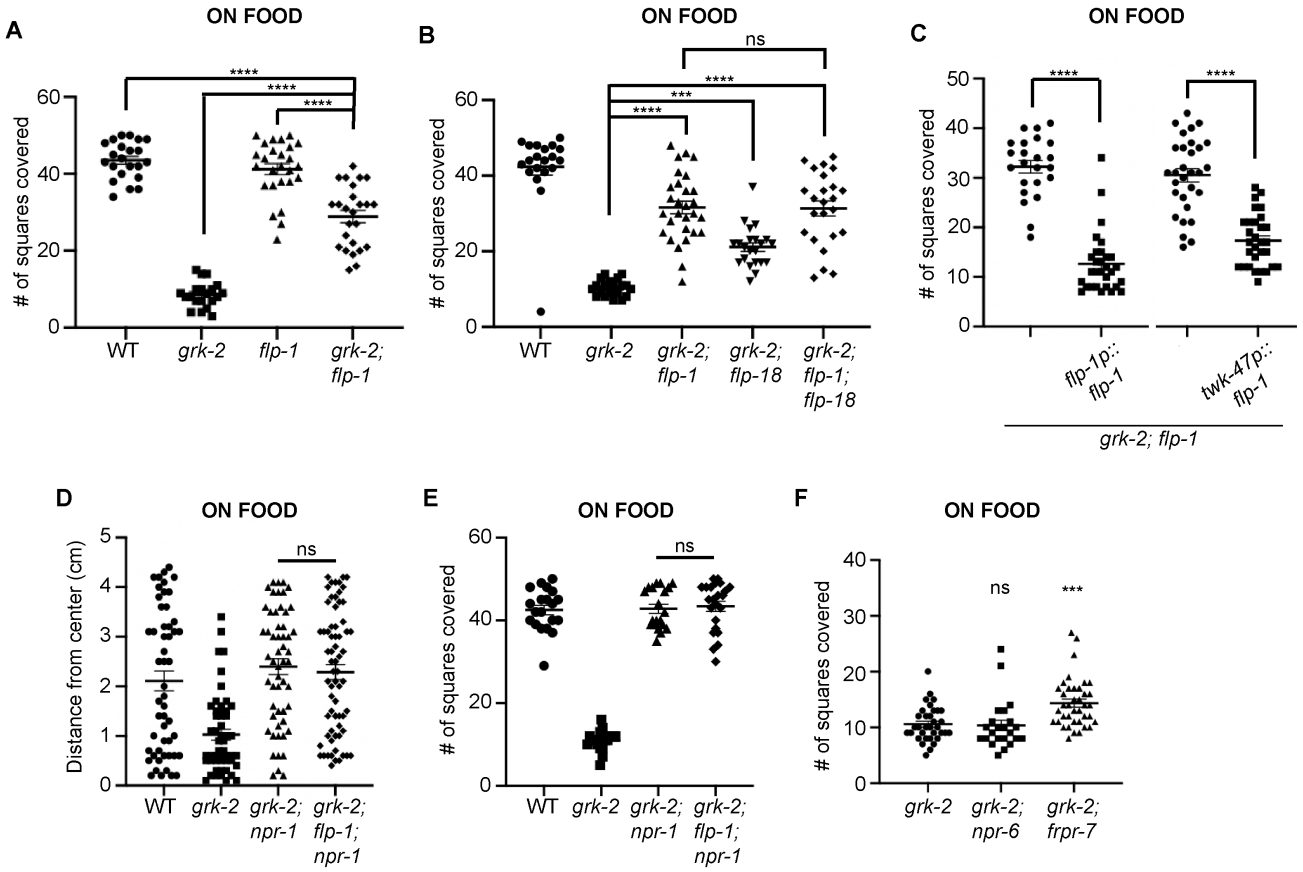
A
ON FOOD
# of squares covered
****
****
****
WT
grk-2
flp-1
grk-2; flp-1
B
ON FOOD
# of squares covered
ns
****
***
****
WT
grk-2
grk-2; flp-1
grk-2; flp-18
grk-2; flp-1; flp-18
C
ON FOOD
# of squares covered
****
****
flp-1p::flp-1
twk-47p::flp-1
grk-2; flp-1
D
ON FOOD
Distance from center (cm)
ns
WT
grk-2
grk-2; npr-1
grk-2; flp-1; npr-1
E
ON FOOD
# of squares covered
ns
WT
grk-2
grk-2; npr-1
grk-2; flp-1; npr-1
F
ON FOOD
# of squares covered
ns
***
grk-2
grk-2; npr-6
grk-2; frpr-7

**Figure 8**

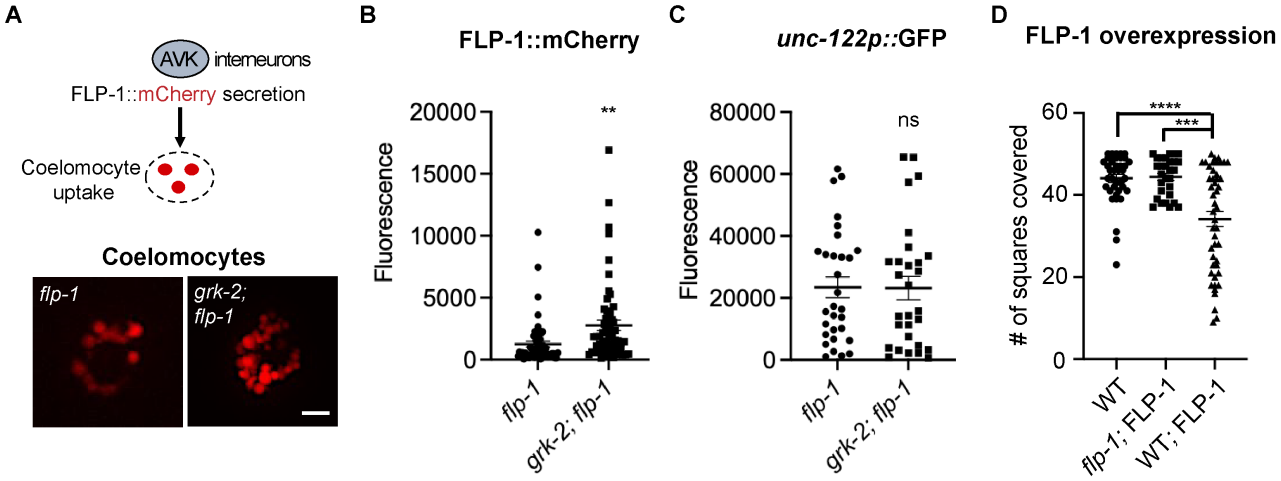
A
AVK
interneurons
FLP-1::mCherry secretion
Coelomocyte uptake
Coelomocytes
flp-1
grk-2; flp-1
B
FLP-1::mCherry
Fluorescence
20000
15000
10000
5000
0
**
flp-1
grk-2; flp-1
C
unc-122p::GFP
Fluorescence
80000
60000
40000
20000
0
ns
flp-1
grk-2; flp-1
D
FLP-1 overexpression
# of squares covered
60
40
20
0
****
***
WT
flp-1; FLP-1
WT; FLP-1

Figure 9

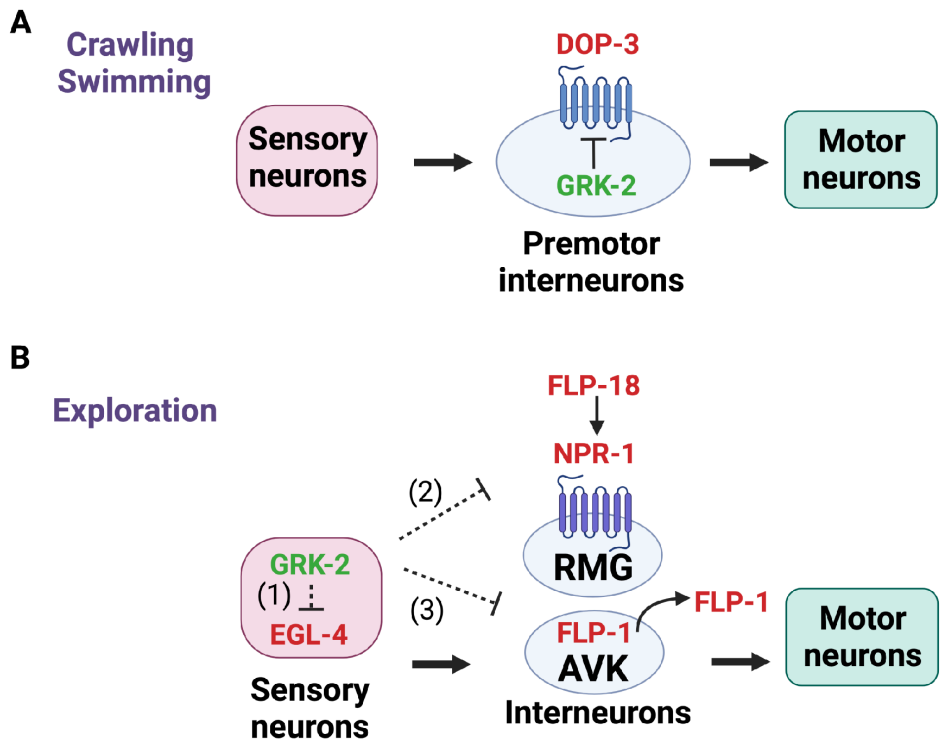
A
Crawling
Swimming
Sensory neurons
DOP-3
GRK-2
Premotor interneurons
Motor neurons
B
Exploration
FLP-18
NPR-1
(2)
(3)
GRK-2
(1)
EGL-4
Sensory neurons
RMG
FLP-1
AVK
FLP-1
Interneurons
Motor neurons